FLUXNET-CH_4 Synthesis Activity: Objectives, Observations, and Future Directions

Sara H. Knox[1,2], Robert B. Jackson[1,3], Benjamin Poulter[4], Gavin McNicol[1], Etienne Fluet-Chouinard[1], Zhen Zhang[5], Gustaf Hugelius[6,7] Philippe Bousquet[8], Josep G. Canadell[9], Marielle Saunois[8], Dario Papale[10], Housen Chu[11], Trevor F. Keenan[11,12], Dennis Baldocchi[12], Margaret S. Torn[11], Ivan Mammarella[13], Carlo Trotta[10], Mika Aurela[14], Gil Bohrer[15], David I. Campbell[16], Alessandro Cescatti[17], Samuel Chamberlain[12], Jiquan Chen[18], Weinan Chen[19], Sigrid Dengel[11], Ankur R. Desai[20], Eugenie Euskirchen[21], Thomas Friborg[22], Daniele Gasbarra[23,24], Ignacio Goded[17], Mathias Goeckede[25], Martin Heimann[25,13], Manuel Helbig[26], Takashi Hirano[27], David Y. Hollinger[28], Hiroki Iwata[29], Minseok Kang[30], Janina Klatt[31], Ken W. Krauss[32], Lars Kutzbach[33], Annalea Lohila[14], Bhaskar Mitra[34], Timothy H. Morin[35], Mats B. Nilsson[36], Shuli Niu[19], Asko Noormets[34], Walter C. Oechel[37,38], Matthias Peichl[36], Olli Peltola[14], Michele L. Reba[39], Andrew D. Richardson[40], Benjamin R. K. Runkle[41], Youngryel Ryu[42], Torsten Sachs[43], Karina V. R. Schäfer[44], Hans Peter Schmid[45], Narasinha Shurpali[46], Oliver Sonnentag[47], Angela C. I. Tang[48], Masahito Ueyama[49], Rodrigo Vargas[50], Timo Vesala[13,51], Eric J. Ward[32], Lisamarie Windham-Myers[52], Georg Wohlfahrt[53], and Donatella Zona[37,54]

[1] Department of Earth System Science, Stanford University, Stanford, CA 94305, USA
[2] Department of Geography, The University of British Columbia, Vancouver, BC, V6T 1Z2, Canada
[3] Woods Institute for the Environment and Precourt Institute for Energy, Stanford, CA 94305, USA
[4] NASA Goddard Space Flight Center, Biospheric Sciences Laboratory, Greenbelt, MD 20771, USA
[5] Department of Geographical Sciences, University of Maryland, MD 20742, USA
[6] Department of Physcial Geography, Stockholm University, SE 10691 Stockholm, Sweden
[7] Bolin Centre for Climate Research, Stockholm University, SE 10691 Stockholm, Sweden
[8] Laboratoire des Sciences du Climat et de l'Environnement, LSCE-IPSL (CEA-CNRS-UVSQ), Université Paris-Saclay 91191 Gif-sur-Yvette, France
[9] Global Carbon Project, CSIRO Oceans and Atmosphere, Canberra, ACT 2601, Australia
[10] DIBAF, Università degli Studi della Tuscia, Largo dell'Università, 01100 Viterbo, Italy
[11] Earth and Environmental Sciences Area, Lawrence Berkeley National Lab, Berkeley, CA 94720, USA
[12] Department of Environmental Science, Policy & Management, UC Berkeley, Berkeley, CA 94720, USA
[13] Institute for Atmosphere and Earth System Research/Physics, PO Box 68, Faculty of Science, FI-00014, University of Helsinki, Finland
[14] Finnish Meteorological Institute, PO Box 503, 00101 Helsinki, Finland
[15] Department of Civil, Environmental & Geodetic Engineering, The Ohio State University, Columbus, OH 43210, USA
[16] School of Science, University of Waikato, Hamilton 3240, New Zealand
[17] European Commission, Joint Research Centre (JRC), Directorate for Sustainable Resources, Ispra 21027, Italy

Early Online Release: This preliminary version has been accepted for publication in *Bulletin of the American Meteorological Society*, may be fully cited, and has been assigned DOI 10.1175/BAMS-D-18-0268.1. The final typeset copyedited article will replace the EOR at the above DOI when it is published.

[18] Department of Geography, Environment, and Spatial Sciences and Center for Global Change and Earth Observations, Michigan State, MI 48824, USA
[19] Key Laboratory of Ecosystem Network Observation and Modeling, Institute of Geographic Sciences and Natural Resources Research, Chinese Academy of Sciences, Beijing 100101, China
[20] Department of Atmospheric and Oceanic Sciences, University of Wisconsin-Madison, Madison, WI 53706, USA
[21] University of Alaska Fairbanks, Institute of Arctic Biology, Fairbanks, AK 99775, USA
[22] Department of Geosciences and Natural Resource Management, University of Copenhagen, Oester Voldgade 10, 1350 Copenhagen K, Denmark
[23] Department of Vegetal Biology, University of Napoli Federico II, Via Foria 223, 80139 Napoli, Italy
[24] CNR Institute for Mediterranean Agricultural and Forest Systems, Ercolano (Napoli), 80056, Italy
[25] Max Planck Institute for Biogeochemistry, Hans-Knoell-Str. 10, 07745 Jena, Germany
[26] School of Geography and Earth Sciences, McMaster University, Hamilton, ON L8S 4K1, Canada
[27] Research Faculty of Agriculture, Hokkaido University, Sapporo 060-8589, Japan
[28] USDA Forest Service, Northern Research Station, Durham, NH 03824, USA
[29] Department of Environmental Sciences, Shinshu University, Matsumoto, Nagano, 390-8621, Japan
[30] National Center for AgroMeteorology, 1, Gwanak-ro, Gwanak-gu, Seoul 08826, South Korea
[31] Karlsruhe Institute of Technology, Institute of Meteorology and Climate Research, Kreuzeckbahnstrasse 19, 82467 Garmisch-Partenkirchen, Germany
[32] U.S. Geological Survey, Wetland and Aquatic Research Center, Lafayette, LA 70506, USA
[33] Institute of Soil Science, Center for Earth System Research and Sustainability, Universität Hamburg, Hamburg 20146, Germany
[34] Department of Ecosystem Science and Management, Texas A&M University, College Station, TX 77843, USA
[35] Department of Environmental Resources Engineering, State University of New York College of Environmental Science and Forestry, Syracuse, NY 13210, USA
[36] Department of Forest Ecology and Management, Swedish University of Agricultural Sciences, Umeå, Sweden
[37] Department of Biology, San Diego State University, San Diego, CA 92182, USA
[38] Department of Physical Geography, University of Exeter, Exeter, UK
[39] United States Department of Agriculture, Agricultural Research Service, Delta Water Management Research Service, Jonesboro, AR 72401, USA
[40] School of Informatics, Computing, and Cyber Systems, and Center for Ecosystem Science and Society, Northern Arizona University, Flagstaff AZ 86004 USA
[41] Department of Biological and Agricultural Engineering, University of Arkansas, Fayetteville, AR, USA
[42] Department of Landscape Architecture and Rural Systems Engineering, Seoul National University, South Korea
[43] GFZ German Research Centre for Geoscience, Telegrafenberg, 14473 Potsdam, Germany
[44] Department of Biological Sciences, 195 University Ave, Rutgers University Newark, Newark, NJ 07102, USA

Accepted for publication in *Bulletin of the American Meteorological Society.* DOI 10.1175/BAMS-D-18-0268.1.

[45] Institute of Meteorology and Climatology – Atmospheric Environmental Research (IMK-IFU), Karlsruhe Institute of Technology (KIT), Kreuzeckbahnstrasse 19, 82467 Garmisch-Partenkirchen, Germany
[46] Biogeochemistry Research Group, Department of Biological and Environment al Sciences, University of Eastern Finland, Kuopio, Finland
[47] Département de Géographie & Centre d'Études Nordiques, 520 Chemin de la Côte Sainte-Catherine, Montréal, QC, H2V 2B8, Canada
[48] Sarawak Tropical Peat Research Institute, Kota Samarahan, Sarawak, Malaysia
[49] Graduate School of Life and Environmental Sciences, Osaka Prefecture University, Japan
[50] Department of Plant and Soil Sciences, University of Delaware, Newark, DE, 19716, USA
[51] Institute for Atmosphere and Earth System Research/Forest Sciences, PO Box 27, Faculty of Agriculture and Forestry, FI-00014, University of Helsinki, Finland
[52] Water Mission Area, U.S. Geological Survey, 345 Middlefield Road, Menlo Park, CA 94025, USA
[53] Department of Ecology, University of Innsbruck, Innsbruck, Austria
[54] Department of Animal and Plant Sciences, University of Sheffield, Sheffield, UK

Corresponding author: Sara Knox (saraknox.knox@gmail.com)

Accepted for publication in *Bulletin of the American Meteorological Society.* DOI 10.1175/BAMS-D-18-0268.1.

Abstract

This paper describes the formation of, and initial results for, a new FLUXNET coordination network for ecosystem-scale methane (CH_4) measurements at 60 sites globally, organized by the Global Carbon Project in partnership with other initiatives and regional flux tower networks. The objectives of the effort are presented along with an overview of the coverage of eddy covariance (EC) CH_4 flux measurements globally, initial results comparing CH_4 fluxes across the sites, and future research directions and needs. Annual estimates of net CH_4 fluxes across sites ranged from -0.2 ± 0.02 g C m^{-2} y^{-1} for an upland forest site to 114.9 ± 13.4 g C m^{-2} y^{-1} for an estuarine freshwater marsh, with fluxes exceeding 40 g C m^{-2} y^{-1} at multiple sites. Average annual soil and air temperatures were found to be the strongest predictor of annual CH_4 flux across wetland sites globally. Water table position was positively correlated with annual CH_4 emissions, although only for wetland sites that were not consistently inundated throughout the year. The ratio of annual CH_4 fluxes to ecosystem respiration increased significantly with mean site temperature. Uncertainties in annual CH_4 estimates due to gap filling and random errors were on average $\pm$ 1.6 g C m^{-2} y^{-1} at 95% confidence, with the relative error decreasing exponentially with increasing flux magnitude across sites. Through the analysis and synthesis of a growing EC CH_4 flux database, the controls on ecosystem CH_4 fluxes can be better understood, used to inform and validate Earth system models, and reconcile differences between land-surface model- and atmospheric-based estimates of CH_4 emissions.

Accepted for publication in *Bulletin of the American Meteorological Society.* DOI 10.1175/BAMS-D-18-0268.1.

Capsule Summary

Here we describe a new coordination activity and initial results for a global synthesis of eddy covariance CH_4 flux measurements.

Accepted for publication in *Bulletin of the American Meteorological Society.* DOI 10.1175/BAMS-D-18-0268.1.

1. Introduction

Atmospheric methane (CH_4) is the second-most important anthropogenic greenhouse gas following carbon dioxide (CO_2) (Myhre et al. 2013). The concentration of CH_4 in the atmosphere today is about 2.5-times higher than in 1750 (Saunois et al. 2016a). The increase in atmospheric CH_4 has arisen from human activities in agriculture, energy production, and waste disposal, and from changes in natural CH_4 sources and sinks (Saunois et al. 2016a, 2017, 2016b; Turner et al. 2019). Based on top-down atmospheric inversions, global CH_4 emissions for the decade of 2003-2012 were an estimated ~420 Tg C y^{-1} (range 405–426 Tg C y^{-1}) (Saunois et al. 2016a). However, some analyses suggest that uncertainties in global CH_4 sources and sinks are higher than those for CO_2, and uncertainties from natural sources exceed those from anthropogenic emissions (Saunois et al. 2016a). In particular, the largest source of uncertainty in the global CH_4 budget is related to emissions from wetlands and inland waters (Saunois et al. 2016a; Melton et al. 2013; Bastviken et al. 2011). Wetland CH_4 emissions may contribute as much as 25-40% of the global total and are a leading source of interannual variability in total atmospheric CH_4 concentrations (Bousquet et al. 2006; Chen and Prinn 2006; Saunois et al. 2016a).

Direct, ground-based measurements of in situ CH_4 fluxes with high measurement frequency are important for understanding the responses of CH_4 fluxes to environmental factors including climate, for providing validation datasets for the land-surface models used to infer global CH_4 budgets, and for constraining CH_4 budgets. Eddy covariance (EC) flux towers measure real-time exchange of gases such as CO_2, CH_4, water vapour, and energy between the land-surface and the atmosphere. The EC technique has emerged as a widespread means of measuring trace gas exchange because it provides direct and near-continuous ecosystem-scale flux measurements without disturbing the soil or vegetation (Baldocchi 2003; Aubinet et al. 2012). There are more

Accepted for publication in *Bulletin of the American Meteorological Society.* DOI 10.1175/BAMS-D-18-0268.1.

than 900 reported active and historical flux tower sites globally and approximately 7000 site-years of data collected (Chu et al. 2017). While most of these sites measure CO_2, water vapour, and energy exchange, the development of new and robust CH_4 sensors has resulted in a rapidly growing number of CH_4 EC measurements (Baldocchi 2014; Morin 2018), primarily in natural and agricultural wetlands (Petrescu et al. 2015).

Since the late-1990s, with a growing number of long-term, near-continuous EC measurements, the EC community has been well coordinated for integrating and synthesizing CO_2, water vapour and energy fluxes. This cross-site coordination resulted in the development of regional flux networks for Europe (EuroFlux, CarboEurope and ICOS), Australia (OzFlux), North and South America (AmeriFlux, Large Biosphere Amazon, Fluxnet-Canada/Canadian Carbon Program, and MexFlux), Asia (AsiaFlux, ChinaFlux, KoFlux, and USCCC), and globally, FLUXNET (Papale et al. 2012; Baldocchi 2014). The resulting FLUXNET database (http://fluxnet.fluxdata.org/) has been used extensively to evaluate satellite measurements, inform Earth system models, generate data-driven CO_2 flux products, and provide answers to a broad range of questions about atmospheric fluxes related to ecosystems, land use and climate (Pastorello et al. 2017). FLUXNET has grown steadily over the past 25 years, enhancing our understanding of carbon, water and energy cycles in terrestrial ecosystems (Chu et al. 2017).

Similar community efforts and syntheses for CH_4 remain limited in part because EC measurements for CH_4 fluxes were rarer until recently. Whereas the earliest EC measurements of CO_2 fluxes date back to the late 1970s and early 1980s (Desjardins 1974; Anderson et al. 1984), the first EC CH_4 flux measurements only began in the 1990s (Verma et al. 1992; Shurpali and Verma 1998; Fan et al. 1992; Kim et al. 1999), with reliable, easy-to-deploy field sensors only becoming available in the past decade or so. EC CH_4 flux measurements became more feasible

Accepted for publication in *Bulletin of the American Meteorological Society.* DOI 10.1175/BAMS-D-18-0268.1.

with advances in sensor development, such as tunable diode laser absorption spectrometers, that allowed researchers to measure previously undetectable trace gas fluxes with higher signal to noise ratios (Rinne et al. 2007; McDermitt et al. 2011). After these new sensors were commercialized, and low power, low maintenance open-path sensors were developed that could be operated by solar panels in remote locations, the number of CH_4 flux tower measurements increased substantially (Baldocchi 2014; Morin 2018). The rapidly growing number of EC CH_4 flux measurements presents new opportunities for FLUXNET-type analyses and syntheses of ecosystem-scale CH_4 flux observations.

This manuscript describes initial results from a new coordination activity for flux tower CH_4 measurements organized by the Global Carbon Project (GCP) in collaboration with regional flux networks and FLUXNET. The goal of the activity is to develop a global database for EC CH_4 observations to answer regional and global questions related to CH_4 cycling. Here, we describe the objectives of the FLUXNET-CH_4 activity, provide an overview of the current geographic and temporal coverage of CH_4 flux measurements globally, present initial analyses exploring time scales of variability, uncertainty, trends and drivers of CH_4 fluxes across 60 sites, and discuss future research opportunities for examining controls on CH_4 emissions and reducing uncertainties in the role of wetlands in the global CH_4 cycle.

2. FLUXNET-CH_4 synthesis objectives and tasks

This activity is part of a larger GCP effort to establish and better constrain the Global Methane Budget (http://www.globalcarbonproject.org/methanebudget/index.htm), and is designed to develop a CH_4 database component in FLUXNET for a global synthesis of CH_4 flux tower data. To this end, we are surveying, assembling, and synthesizing data from the EC

Accepted for publication in *Bulletin of the American Meteorological Society.* DOI 10.1175/BAMS-D-18-0268.1.

community, in coordination with regional networks, including AmeriFlux's 2019 'Year of Methane' (http://ameriflux.lbl.gov/year-of-methane/year-of-methane/), FLUXNET initiatives, and other complementary activities. In particular, this work is being carried out in parallel with the European Union's Readiness of ICOS for Necessities of Integrated Global Observations (RINGO) project which is working to standardize protocols for flux calculations, quality control and gap-filling for CH_4 fluxes (Nemitz et al. 2018). Methane-specific protocols are needed because of the added complexities and high variability of CH_4 flux measurements and dynamics (Nemitz et al. 2018).

Our approach is to include all currently available and future CH_4 flux tower observations in a global CH_4 database, including freshwater, coastal, natural and managed ecosystems, as well as upland ecosystems that may be measuring CH_4 uptake by soils. The initiative is open to all members of the EC community. Database compilation began in 2017 and is ongoing. Data from sites in the Americas can be submitted to AmeriFlux (http://ameriflux.lbl.gov/data/how-to-uploaddownload-data/); otherwise, data can be submitted to the European Fluxes Database Cluster (http://www.europe-fluxdata.eu/home/sites-list).

In addition to many applications, an ultimate goal of the FLUXNET-CH_4 activity is to generate a publicly available, open-access, data-driven global CH_4 emissions product using similar machine-learning-based approaches used for CO_2 fluxes (Jung et al. 2009; Tramontana et al. 2016). The product will be based on mechanistic factors associated with CH_4 emissions and new spatio-temporal information on wetland area and dynamics for constraining CH_4-producing areas. This gridded product will provide an independent bottom-up estimate of global wetland CH_4 emissions to compare with estimates of global CH_4 emissions from land-surface models and atmospheric inversions. Recent work has shown the potential to upscale EC CH_4 flux

Accepted for publication in *Bulletin of the American Meteorological Society.* DOI 10.1175/BAMS-D-18-0268.1.

observations across northern wetlands, with predictive performance comparable to previous studies upscaling net CO_2 exchange (Peltola et al. 2019), however, our focus is on a globally gridded product.

The near continuous, high-frequency nature of EC measurements also offers significant promise for improving our understanding of ecosystem-scale CH_4 flux dynamics. As such, this synthesis also aims to investigate the dominant controls on net ecosystem-scale CH_4 fluxes from hourly to interannual time scales across wetlands globally, and to characterize scale-emergent, nonlinear, and lagged processes of CH_4 exchange.

Methane is produced during decomposition under anaerobic or reducing conditions and is transported to the atmosphere via plant-mediated transport, ebullition and diffusion (Bridgham et al. 2013). During transport, CH_4 can pass through unsaturated soil layers and be consumed or oxidized by aerobic bacteria (Wahlen 1993). Process-based biogeochemical models developed and applied at site, regional and global scales simulate these individual processes with varying degrees of complexity (Bridgham et al. 2013; Melton et al. 2013; Poulter et al. 2017; Castro-Morales et al.; Grant and Roulet 2002). The large range in predicted wetland CH_4 emissions rates suggests that there is both substantial parameter and structural uncertainty in large-scale CH_4 flux models, even after accounting for uncertainties in wetland areas (Poulter et al. 2017; Saunois et al. 2016a; Melton et al. 2013; Riley et al. 2011). A global EC CH_4 database and associated environmental variables can help constrain the parameterization of process-based biogeochemistry models (Saunois et al. 2016a; Bridgham et al. 2013; Oikawa et al. 2017). Furthermore, a key challenge is evaluating globally-applicable process-based CH_4 models at a spatial scale comparable to model grid cells (Melton et al. 2013; Riley et al. 2011). A globally gridded wetland CH_4 emissions product upscaled from EC fluxes can help resolve this issue by

Accepted for publication in *Bulletin of the American Meteorological Society.* DOI 10.1175/BAMS-D-18-0268.1.

providing a scale appropriate model evaluation dataset. As such, the global CH_4 database and gridded product will also be used to parameterize and benchmark the performance of land-surface models of global CH_4 emissions, providing a unique opportunity for informing and validating biogeochemical models.

3. Methods

Based on a survey of the EC community (announced via the fluxnet-community@george.lbl.gov and AmeriFlux-Community@lbl.gov listservs), information available in regional networks and FLUXNET, and the scientific literature, we estimate that at least 200 sites worldwide are currently applying the EC method for CH_4 flux measurements (Figure 1). Here we focus on findings from across 60 of the ~110 sites currently committed to participating in our FLUXNET-CH_4 activity (Tables A1 and S1). Data from this initial set of sites were selected because they were publicly available or were contributed directly by site PIs. We will continue to engage the EC community more broadly and expand the database in the future.

3.1. Data standardization, gap-filling, and partitioning

We used similar data processing procedures as FLUXNET to standardize and gap-fill measurements, and in the case of net CO_2 exchange, partition fluxes across sites (http://fluxnet.fluxdata.org/data/aboutdata/data-processing-101-pipeline-and-procedures/). Standard quality assurance and quality control of the data was first performed by site PIs. In nearly all cases, data collected by the local tower teams were first submitted to the data archives hosted by the regional flux networks, where data are pre-screened and formatted based on the

Accepted for publication in *Bulletin of the American Meteorological Society.* DOI 10.1175/BAMS-D-18-0268.1.

regional network data protocols. Data from the regional networks then entered our flux processing procedure.

Within our processing procedure, data were first checked for obvious problems including unit errors, spikes, and out-of-range values based on visualization of the data and statistical metrics. Next, the data were filtered, gap-filled and partitioned. Friction velocity (u_*) filtering, based on relating night-time CO_2 fluxes to u_*, was implemented using the REddyProc package (Wutzler et al. 2018) for R statistical software (R Development Core Team, 2018, version 3.5.0), although in a few cases u_* filtering was performed by the site PIs. Gaps in meteorological variables including air temperature (TA), incoming shortwave (SW_{IN}) and longwave (LW_{IN}) radiation, vapour pressure deficit (VPD), pressure (PA), precipitation (P), and windspeed (WS) were filled with ERA-Interim (ERA-I) reanalysis data (Vuichard and Papale 2015). Gaps in CO_2 and latent and sensible heat fluxes were filled using the marginal distribution sampling method (Reichstein et al. 2005) using the REddyProc package (Wutzler et al. 2018). Net CO_2 fluxes were partitioned into gross primary production (GPP) and ecosystem respiration (ER) using both the nighttime (Reichstein et al. 2005) and daytime (Lasslop et al. 2010) approaches also implemented in REddyProc (Wutzler et al. 2018).

There are as yet no standards for gap-filling CH_4 flux measurements and this is an active and ongoing area of research (Nemitz et al. 2018). Gaps in CH_4 fluxes were filled using artificial neural networks (ANNs), as they have shown good performance for gap-filling CH_4 flux data (Dengel et al. 2013; Knox et al. 2015; Morin et al. 2014a; Nemitz et al. 2018; Goodrich et al. 2015). Details of the ANN routine are provided in Knox et al. (2016) and are summarized here briefly. The ANN routine was optimized for both generalizability and representativeness. To facilitate representativeness, explanatory data were divided into a maximum of 15 data clusters

Accepted for publication in *Bulletin of the American Meteorological Society.* DOI 10.1175/BAMS-D-18-0268.1.

using the k-means algorithm. To avoid biasing toward conditions with better flux data coverage (e.g. summer and daytime), data used to train, test, and validate the ANN were proportionately sampled from these clusters. Several neural network architectures of increasing complexity were tested, ranging from one hidden layer with the number of nodes equal to the number of explanatory data variables (N) to two hidden layers with 1.5N and 0.75N nodes, respectively. The architecture of each neural network was initialized 10 times with random starting weights, and the initialization resulting in the lowest mean sampling error was selected. The simplest architecture, whereby additional increases in complexity resulted in <5% reduction in mean squared error, was chosen and the prediction saved. This procedure was repeated with 20 resamplings of the data, and missing half hours were filled using the median prediction. A standard set of variables available across all sites were used to gap-fill CH_4 fluxes (Dengel et al. 2013), including TA, SW_{IN}, WS, PA, and sine and cosine functions to represent seasonality. These meteorological variables were selected since they are relevant to CH_4 exchange and were gap-filled using the ERA-I reanalysis data. Other variables related to CH_4 exchange such as water table depth (WTD) or soil temperature (TS) were not included as explanatory variables as they were not available across all sites or had large gaps that could not be filled using the ERA-I reanalysis data. These missing data for variables highlight some of the key challenges in standardizing CH_4 gap-filling methods across sites and emphasize the need for standardized protocols of auxiliary measurements across sites (c.f. 'Future research directions and needs') (Nemitz et al. 2018; Dengel et al. 2013). ANN gap-filling was performed using MATLAB (MathWorks Inc., 2018, version 9.4.0).

Annual CH_4 budgets represent gap-filled, half-hourly fluxes integrated over an entire year or growing season. If fluxes were only measured during the growing season, we assumed that

Accepted for publication in *Bulletin of the American Meteorological Society.* DOI 10.1175/BAMS-D-18-0268.1.

fluxes outside of this period were negligible, although we acknowledge that cold season fluxes can account for as much as ~13-50% of the annual CH_4 emissions in some locations (Zona et al. 2016; Treat et al. 2018b; Helbig et al. 2017a; Kittler et al. 2017).

3.2. Uncertainty estimation

ANNs were also used to estimate annual gap-filled and random uncertainty in CH_4 flux measurements (Richardson et al. 2008; Moffat et al. 2007; Anderson et al. 2016; Knox et al. 2018). Here, we focus on assessing the random error, but a full assessment of total flux measurement error also requires quantifying systematic error or bias (Baldocchi 2003). Systematic errors, due to incomplete spectral response, lack of nocturnal mixing, sub-mesoscale circulations, and other factors are discussed elsewhere (Baldocchi 2003; Peltola et al. 2015) and are the focus of other ongoing initiatives.

Random errors in EC fluxes follow a double exponential (Laplace) distribution with a standard deviation varying with flux magnitude (Richardson et al. 2012, 2006). Model residuals of gap-filling algorithms such as ANNs provide a reliable, and conservative 'upper limit', estimate of the random flux uncertainty (Moffat et al. 2007; Richardson et al. 2008). For half-hourly CH_4 flux measurements, random error was estimated using the residuals of the median ANN predictions. At each site, the probability density function (PDF) of the random flux measurement error more closely followed a double-exponential (Laplace) rather than normal (Gaussian) distribution, with the root-mean-square error (RMSE) for the Laplace distribution fitted to the PDF of random errors consistently lower than the normal distributed error. From half-hourly flux measurements, random error can also be estimated using the daily differencing approach (Richardson et al. 2012). Random error estimates ($\sigma(\delta)$), as expressed as the standard

Accepted for publication in *Bulletin of the American Meteorological Society.* DOI 10.1175/BAMS-D-18-0268.1.

deviation of the double-exponential distribution with scaling parameter β, where $\sigma(\delta) = \sqrt{2}\beta$ (Richardson et al. 2006), were found to be nearly identical using the two approaches ($\sigma(\delta)_{model\ residual} = 1.0 \times \sigma(\delta)_{daily\ differencing} + 1.21$), $r^2 = 0.97$, $p < 0.001$), supporting the use of the model residual approach for estimating random error. As discussed below, $\sigma(\delta)$ scaled linearly with the magnitude of CH_4 fluxes at nearly all sites. To quantify random uncertainty of cumulative fluxes, we used a Monte Carlo simulation that randomly draws 1,000 random errors for every original measurement using $\sigma(\delta)$ binned by flux magnitude, and then computed the variance of the cumulative sums (Anderson et al. 2016). For gap-filled values, the combined gap-filling and random uncertainty was calculated from the variance of the cumulative sums of the 20 ANN predictions (Anderson et al. 2016; Oikawa et al. 2017; Knox et al. 2015). The annual cumulative uncertainty at 95% confidence was estimated by adding the cumulative gap-filling and random measurement uncertainties in quadrature (Richardson and Hollinger 2007; Anderson et al. 2016). Note that when reporting mean or median annual CH_4 fluxes across sites, error bars represent the standard error.

3.3. Wavelet-based timescale decomposition

Methane fluxes are highly dynamic and vary across a range of time scales (Sturtevant et al. 2016; Koebsch et al. 2015). For example, in wetlands with permanent inundation, the seasonal variation of CH_4 exchange is predominantly controlled by temperature and plant phenology (Chu et al. 2014; Sturtevant et al. 2016). Ecosystem CH_4 exchange also varies considerably at both longer (e.g. interannual; (Knox et al. 2016; Rinne et al. 2018)) and shorter (e.g. weeks, days or hours; (Koebsch et al. 2015; Hatala et al. 2012; Schaller et al. 2018)) time scales. Wavelet decomposition is a particularly useful tool for investigating scale in geophysical

Accepted for publication in *Bulletin of the American Meteorological Society.* DOI 10.1175/BAMS-D-18-0268.1.

and ecological analysis (Cazelles et al. 2008; Torrence and Compo 1998), because it can characterize both the time scale and location of patterns and perturbations in the data. Partitioning variability across temporal scales can help to isolate and characterize important processes (Schaller et al. 2018).

The maximal overlap discrete wavelet transform (MODWT) was used to decompose the time scales of variability in gap-filled CH_4 flux measurements, as described in Sturtevant et al. (2016). The MODWT allows the time series to be decomposed into the detail added from progressively coarser to finer scales and either summed or treated individually to investigate patterns across scales. We reconstructed the detail in the fluxes for dyadic scales 1 (2^1 measurements = 1h) to 14 (2^{14} measurements = 341 days). Since patterns generated by ecological processes tend to occur over a scale range rather than at one individual scale, the detail over adjacent scales were summed to analyze four general time scales of variation (Sturtevant et al. 2016). These time scales included the 'hourly' scale (1-2 h) representing perturbations such the passage of clouds overhead and turbulent scales up to the spectral gap, the 'diel' scale (4 h to 1.3 days) encompassing the diel cycles in sunlight and temperature, the 'multiday' scale (2.7 to 21.3 days) reflecting synoptic weather variability or fluctuations in water levels, and the 'seasonal' scale (42.7 to 341 days) representing the annual solar cycle and phenology. Data were wavelet decomposed into the hourly, diel, and multiday scales using the WMTSA Wavelet Toolkit in MATLAB.

3.4. Statistical analysis

We tested for significant relationships between log-transformed annual CH_4 emissions and a number of covariates using linear mixed-effects models as described in Treat et al.

Accepted for publication in *Bulletin of the American Meteorological Society.* DOI 10.1175/BAMS-D-18-0268.1.

(2018b). The predictor variables of CH_4 flux we evaluated included: biome or ecosystem type (categorical variables), and continuous biophysical variables including mean seasonal WTD, mean annual soil and air temperature (T_{MST} and T_{MAT}, respectively), net ecosystem exchange (NEE), GPP, and ER. When considering continuous variables, we focused on freshwater wetlands for comparison with previous CH_4 synthesis activities. Soil temperature was measured between 2 cm and 25 cm below the surface in different studies. The results below are presented for GPP and ER covariates that are partitioned using the nighttime flux partitioning algorithm (Wutzler et al. 2018; Reichstein et al. 2005), although similar findings were obtained using daytime partitioned estimates. Additionally, individual sites or site years were excluded when gaps in measurements exceeded two consecutive months, which explains the differences in the number of sites and site years in Section 4.3 below.

Mixed-effects modeling was used because of the potential bias of having measurements over several years, with site included as a random effect in the analysis (Treat et al. 2018b). The significance of individual predictor variables was evaluated using a χ^2 test against a null model using only site as a random variable (Bates et al. 2015), with both models fit without reduced maximum likelihood. For multiple linear regression models, we used the model selection process outlined in Zuur et al. (2009). To incorporate annual cumulative uncertainty when assessing the significance of trends and differences in annual CH_4 fluxes across biomes and ecosystem types, we used a Monte Carlo simulation that randomly draws 1,000 annual cumulative uncertainties for each estimate of annual CH_4 flux. For each random draw the significance of the categorical variable was tested using a χ^2 test against the null model with only site as a random variable. We report the marginal r^2 (r_m^2) which describes the proportion of variance explained by the fixed

Accepted for publication in *Bulletin of the American Meteorological Society.* DOI 10.1175/BAMS-D-18-0268.1.

409 factors alone (Nakagawa and Schielzeth 2013). The mixed-effects modeling was implemented
410 using the lmer command from the lme4 package (Bates et al. 2014) for R statistical software.
411
412 **4. Results and discussion**
413 *4.1. Geographic and temporal coverage of eddy covariance CH_4 flux measurements*
414 We identified 200 sites worldwide that are applying the EC method for CH_4 (Figure 1;
415 Table S1); wetlands (including natural, managed and restored wetlands) comprise the majority of
416 sites (59%), with rice agriculture (10%) as the second most represented vegetation type. The
417 predominance of wetland and rice paddy sites in the database is unsurprising because many
418 studies are designed to target ecosystems expected to have relatively large CH_4 emissions.
419 However, there are also sites in ecosystems that are typically smaller sources or even sinks of
420 CH_4 such as upland forests (13%) and grasslands (8%). Additionally, six sites (~3%) are urban,
421 with another five sites measuring CH_4 fluxes from open water bodies. Although identified sites
422 span all continents except Antarctica, the majority are concentrated in North America and
423 Europe, with a growing number of sites in Asia (Figure 1; Table S1).
424 Measurements of CH_4 fluxes cover a broad range of climates and a large fraction of wetland
425 habitats (Figure 2), with the tropics and tropical wetlands notably underrepresented. As discussed
426 below (see Future research directions and needs), one important goal of FLUXNET and the
427 regional networks is to increase site representativeness and extend measurements in under-
428 sampled regions. Increasing the number of tropical sites is particularly important for CH_4
429 because more than half of global CH_4 emissions are thought to come from this region (Saunois et
430 al. 2016a; Dean et al. 2018). Furthermore, compared to northern wetlands, their biogeochemistry
431 remains relatively poorly understood (Mitsch et al. 2009; Pangala et al. 2017). We expect the

Accepted for publication in *Bulletin of the American Meteorological Society.* DOI 10.1175/BAMS-D-18-0268.1.

number of CH_4 flux sites and their geographic and temporal coverage to continue to increase, as has occurred through time for CO_2, water vapour, and energy flux measurements in FLUXNET (Pastorello et al. 2017; Chu et al. 2017).

Long-term CH_4 flux time series are key to understanding the causes of year-to-year variability and trends in fluxes (Chu et al. 2017; Euskirchen et al. 2017; Pugh et al. 2018). The longest continuous record of CH_4 flux measurements, from a fen in Finland (Rinne et al. 2018), is now ~14 years and ongoing (Table S1). Three other sites have measurements exceeding 10 years; however, the median length is 5 years, with most sites established from 2013 onward (Table S1). Longer time series are also important for both exploring the short- and long-term effects of extreme events on fluxes and tracking the response of disturbed or restored ecosystems over time (Pastorello et al. 2017). Furthermore, they can help address new and emerging science questions, such as quantifying CH_4 feedbacks to climate with rising temperatures and associated changes in ecosystem composition, structure and function (Helbig et al. 2017a,b; Dean et al. 2018), and the role of wetland emissions in atmospheric CH_4 variability (McNorton et al. 2016; Poulter et al. 2017).

4.2. CH_4 fluxes and trends across biomes and ecosystem types

Half-hourly and annual net CH_4 fluxes for the 60 sites currently included in the database exhibited strong variability across sites (Figure 3 and Figure 4). Across the dataset, the mean half-hourly CH_4 flux was greater than the median flux, indicating a positively skewed distribution with infrequent, large emissions (Figure 3a), similar to findings from chamber-based syntheses (Olefeldt et al. 2013; Turetsky et al. 2014). Mean and median CH_4 fluxes were smaller at higher latitudes and larger at lower latitudes (Figure 3b), comparable again to trends in CH_4

Accepted for publication in *Bulletin of the American Meteorological Society.* DOI 10.1175/BAMS-D-18-0268.1.

fluxes observed in predominantly chamber-based syntheses (Bartlett and Harriss 1993; Turetsky et al. 2014; Treat et al. 2018b).

The continuous nature of EC flux measurements is well suited for quantifying annual ecosystem-scale CH_4 budgets, along with accumulated uncertainty (c.f. Section 4.5). Annual estimates of net CH_4 flux for each of the 60 sites in the flux tower database ranged from -0.2 ± 0.02 g C m^{-2} y^{-1} for an upland forest site to 114.9 ± 13.4 g C m^{-2} y^{-1} for an estuarine freshwater marsh (Rey-Sanchez et al. 2018), with fluxes exceeding 40 g C m^{-2} y^{-1} at multiple sites (Figure 4b). These emissions are of a considerably broader range and have much higher annual values than in an earlier synthesis by Baldocchi (2014) which included published values from 13 sites (Figure 4a); median annual CH_4 fluxes (± SE) in that study were 6.4 ± 1.9 g C m^{-2} y^{-1}, compared with 10.0 ± 1.6 g C m^{-2} y^{-1} for our expanded database. Annual CH_4 sums in our database were positively skewed, with skewness increasing with additional observations due largely to the inclusion of high CH_4-emitting freshwater marsh sites (Figure 4).

As suggested from Figure 3b, annual wetland CH_4 emissions differed significantly among biomes, even when considering accumulated uncertainty (average Monte Carlo χ^2 = 13.4 (12.1-14.7, 95% confidence interval), $df = 3$, $p < 0.05$) (Table 1). Median CH_4 emissions were significantly lower for tundra wetlands (2.9 ± 1.3 g C m^{-2} y^{-1}) than temperate wetlands (27.4 ± 3.4 g C m^{-2} y^{-1}). Higher CH_4 emissions were observed from subtropical/tropical wetlands (43.2 ± 11.2 g C m^{-2} y^{-1}), based on only three site years of data, however, emphasizing the need for additional flux tower measurements in the tropics.

Whereas annual boreal/taiga wetland CH_4 emissions were comparable to values reported in a recent synthesis of predominantly chamber-based CH_4 flux measurements (Treat et al. 2018b), our tower-based measurements are ~50% lower and over six times higher for tundra and

Accepted for publication in *Bulletin of the American Meteorological Society.* DOI 10.1175/BAMS-D-18-0268.1.

478 temperate wetlands, respectively (Table 1). The inconsistencies highlighted in Table 1 not only
479 reflect the differences in the number and location of sites between datasets, but also the
480 discrepancies resulting from different measurement techniques. Several studies have noted
481 considerable differences in CH_4 emissions measured using EC and chamber techniques, with
482 estimates from chambers often higher than those from the EC measurements (Schrier-Uijl et al.;
483 Hendriks et al. 2010; Meijide et al. 2011; Krauss et al. 2016). This distinction highlights the need
484 for additional studies investigating the systematic differences caused by the different spatial and
485 temporal sampling footprints of these methods (Krauss et al. 2016; Morin et al. 2017; Windham-
486 Myers et al. 2018; Xu et al. 2017). Characterizing discrepancies between measurement
487 techniques may also help constrain bottom-up estimates of CH_4 emissions and reduce the
488 disagreement of ~15 Tg C y^{-1} between bottom-up (139 Tg CH_4 y^{-1}) and top-down (125 Tg CH_4
489 y^{-1}) estimates of CH_4 emissions from natural wetlands (Saunois et al. 2016a).
490 Annual CH_4 emissions also differed significantly across ecosystems (average Monte
491 Carlo χ^2 = 45.5 (39.3-50.1), df = 9, p < 0.001; Figure 5), with median fluxes highest for
492 freshwater marshes (43.2 ± 4.2 g C m^{-2} y^{-1}) and lowest for upland ecosystems (1.3 ± 0.7 g C m^{-2}
493 y^{-1}). Treat et al. (2018b) also observed the highest annual emissions in marshes and reported a
494 similar median value for temperate marshes (49.6 g C m^{-2} y^{-1}). Wet tundra and bogs had
495 significantly lower annual emissions than marshes (Figure 5), which in part reflects their
496 presence in colder boreal and tundra systems, as well as differences in vegetation type, nutrient
497 status and hydrological regime (Treat et al. 2018b). Low median CH_4 emission was observed
498 from salt marshes in our dataset (0.8 ± 2.9 g C m^{-2} y^{-1}), because high sulfate concentrations
499 inhibit methanogenesis (Poffenbarger et al. 2011; Holm et al. 2016). Even drained wetlands
500 converted to agricultural land can be large sources of CH_4 associated with seasonal flooding

Accepted for publication in *Bulletin of the American Meteorological Society.* DOI 10.1175/BAMS-D-18-0268.1.

(Figure 5). Median annual CH_4 flux from rice was 12.6 ± 1.6 g C m^{-2} y^{-1}, which is slightly lower than the IPCC default value of 15 g C m^{-2} y^{-1} (Sass 2003).

4.3 Environmental controls on annual CH_4 emissions across freshwater wetland sites

Using an integrated CH_4 flux database, we can begin to investigate the factors associated with varying CH_4 emissions across sites. We explored the effects of WTD, T_{MST} or T_{MAT}, NEE, GPP and ER on annual CH_4 flux. At global scales, T_{MAT} and T_{MST} were the most important predictors of annual CH_4 flux across wetland sites ($p < 0.001$ for each), with the fixed factor of T_{MAT} or T_{MST} explaining ~65% of the variation in log transformed annual CH_4 emission (Figure 6a,b). Previous synthesis studies also observed a significant, but weaker, relationship between soil temperature and average CH_4 emissions across sites, explaining < 15% of the variation in CH_4 flux in those studies (Olefeldt et al. 2013; Yvon-Durocher et al. 2014). However, our findings are consistent with numerous site-level studies that report a strong correlation between wetland CH_4 emissions and temperature, with nearly 95% of all EC studies reporting a significant relationship between temperature and CH_4 flux (Morin 2018). Across sites, Peltola et al. (2019) found that the most important predictor in a random forest model used to upscale EC CH_4 emissions across northern latitudes was temperature, again highlighting the importance of temperature in regulating CH_4 emissions within and across sites.

Water table depth has also commonly been identified as a key control on CH_4 emissions (Turetsky et al. 2014; Bubier et al. 2005), because higher water levels often inhibit oxygen availability and lower the soil reduction potential, making methanogenesis more thermodynamically favorable. Although predominantly chamber-based wetland CH_4 syntheses have found a positive relationship between WTD and average or annual CH_4 emissions across

Accepted for publication in *Bulletin of the American Meteorological Society.* DOI 10.1175/BAMS-D-18-0268.1.

sites (Olefeldt et al. 2013; Turetsky et al. 2014; Treat et al. 2018b), we observed no significant relationship between mean WTD and annual CH_4 flux across all sites ($\chi^2 = 0.2$, $df = 1$, $p = 0.66$, $N_{sites} = 20$, $N_{site\ yrs} = 46$), even when considering WTD^2 or WTD^3 (Olefeldt et al. 2013). However, if we consider only sites where WTD was below the soil surface for part or all of the year (Figure 6c solid circles), we did observe a significant relationship with WTD ($p < 0.05$). Conversely, CH_4 emissions for permanently inundated sites showed no significant relationship with WTD (Figure 6c open circles) ($\chi^2 = 0.5$, $df = 1$, $p = 0.50$, $N_{sites} = 13$, $N_{site\ yrs} = 19$). This result supports the finding that wetlands that are permanently inundated or exhibit little variation in WTD tend to show weak to no correlation between WTD and CH_4 emissions (Chu et al. 2014; Jackowicz-Korczyński et al. 2010; Rinne et al. 2007; Christensen et al. 2003); in contrast, wetlands with lower and more variable water levels often have a significant relationship between WTD and CH_4 emissions (Bubier et al. 2005; Treat et al. 2007). However, only half of the sites currently included in the database report water table position, and given the importance of WTD in regulating CH_4 exchange, it is critical to ensure that WTD is measured across all sites.

Gross primary production and ER were both significant positive predictors of annual CH_4 flux ($\chi^2 = 21.3$, $df = 1$, $p < 0.001$, $r_m^2 = 0.29$ and $\chi^2 = 17.1$, $df = 1$, $p < 0.001$, $r_m^2 = 0.25$, respectively, $N_{sites} = 26$, $N_{site\ yrs} = 64$), although there was no significant relationship between NEE and annual CH_4 flux ($\chi^2 = 0.9$, $df = 1$, $p = 0.33$, $N_{sites} = 2$, $N_{site\ yrs} = 64$). However, when considering GPP or ER in a multiple linear regression model with T_{MST}, including interaction terms (Chu et al. 2014), neither GPP nor ER were significant, suggesting that the observed relationship with GPP or ER was due to co-variation with soil temperature and, possibly, other environmental drivers.

Accepted for publication in *Bulletin of the American Meteorological Society.* DOI 10.1175/BAMS-D-18-0268.1.

546 The strong temperature dependence of ecosystem-scale CH_4 emissions we observed across
547 wetland sites is in line with the high temperature sensitivity of CH_4 emissions found across
548 microbial to ecosystem scales (Yvon-Durocher et al. 2014). CH_4 emissions also have a higher
549 temperature dependence than ER, such that the ratio of CH_4 to CO_2 emissions was found to
550 increase markedly with seasonal increases in temperature (Yvon-Durocher et al. 2014).
551 Similarly, we observed a significant increase in the ratio of annual CH_4 to ER along geographic
552 temperature gradients, ranging from 0.4 to 7.9%, with a median value of 2.8% across the dataset
553 (Figure 6d). This relationship suggests that warming may result in a greater relative contribution
554 of CH_4 to total carbon emissions from wetland ecosystems. With a growing FLUXNET CH_4
555 database, it will be possible to further explore the dominant controls on CH_4 fluxes within and
556 across ecosystem types, as well as further investigate the temperature dependence of ecosystem-
557 scale CH_4 exchange (Schipper et al. 2014; Arcus et al. 2016; Yvon-Durocher et al. 2014).
558
559 *4.4 Time scales of variability*
560 Methane fluxes exhibited strong variability over a range of time scales, with the variation
561 across time scales differing between wetland types (Figure 7). As observed previously
562 (Sturtevant et al. 2016), the seasonal time scale dominated CH_4 flux variability across wetland
563 types, but was most pronounced in rice paddies, which have a distinct growing season, and least
564 pronounced in bogs (Figure 7). Across ecosystem types, variation was lowest at the multiday
565 scale, although multiday CH_4 flux variation was slightly greater in rice paddies and wet tundra,
566 potentially indicating greater water table fluctuations (Sturtevant et al. 2016), particularly at rice
567 paddy sites which are subject to seasonal drainage (Knox et al. 2016; Runkle et al. 2019).
568 Whereas some studies report a strong diel pattern in CH_4 emissions from wetlands and rice

Accepted for publication in *Bulletin of the American Meteorological Society.* DOI 10.1175/BAMS-D-18-0268.1.

paddies (Knox et al. 2016; Chu et al. 2014; Morin et al. 2014b; Kim et al. 1999), others have found little or no diel variation (Rinne et al. 2018; Jackowicz-Korczyński et al. 2010; Yagi and Minami 1990; Nadeau et al. 2013). Across wetland types, diel variation was greatest in freshwater marshes (Figure 7), which is consistent with the observations that the vegetation at sites with a strong diel cycle of CH_4 emissions is typically dominated by species with convective gas flow such as *Phragmites australis* or *Typha* spp. (Brix et al. 1992; Chanton et al. 1993). Bogs, fens, and wet tundra showed the greatest variation at the hourly scale (Figure 7). This is likely in part due to typically lower fluxes at these sites as hourly perturbations of turbulent time series are largely dominated by noise (Hollinger and Richardson 2005), as well as the fact that near-surface turbulence and short-term pressure fluctuations can strongly influence CH_4 exchange in these peat dominated ecosystems (Nadeau et al. 2013; Sachs et al. 2008).

4.5 Gap-filling performance and uncertainty quantification

The performance of the neural networks varied strongly across sites (Figure 8). Model r^2, calculated from the median ANN prediction and observed fluxes at each site, ranged from ~0 to 0.92 across sites, with a median value of 0.41. Across sites, ANN performance was strongly linked to the percentage of total variance at diel and seasonal scales ($r^2 = 0.69$, $p < 0.001$), indicating that across the wide range of observed flux magnitudes, sites with a more distinct seasonal and diel pattern tended to be more predictable (Figure 8). There was also a significant negative relationship between model r^2 and the percentage of total variance at the hourly scale across sites ($r^2 = 0.72$, $p < 0.001$), because, as noted previously, hourly perturbations are largely dominated by noise (Hollinger and Richardson 2005).

Accepted for publication in *Bulletin of the American Meteorological Society.* DOI 10.1175/BAMS-D-18-0268.1.

Knowledge of the random errors in half-hourly flux measurements is not only important for evaluating the uncertainty in cumulative fluxes (e.g. daily, monthly, or annual) and comparing fluxes across tower sites, but it also needed to incorporate information about random flux errors in model-data synthesis activities (Richardson et al. 2006). As noted above, random flux error more closely followed a Laplace rather than Gaussian distribution. Within sites, $\sigma(\delta)$ was not constant, but rather nearly always scaled with the magnitude of CH_4 fluxes (Figure 9a), as predicted from theory (Richardson et al. 2006). As observed for other fluxes (Richardson et al. 2006), both the slope and intercept of this relationship varied among sites, and depending on the sign of the flux (Figure 9a). Across sites, random flux error therefore scaled linearly with the magnitude of mean CH_4 flux ($r^2 = 0.86$, $p < 0.001$), even when excluding the two highest CH_4-emitting sites ($r^2 = 0.46$, $p < 0.001$) (Figure 9b). Whereas closed-path CH_4 analyzers have been found to have lower random errors and instrument noise compared with open-path sensors (Peltola et al. 2014), there was no clear evidence of a systematic effect of the influence of closed- vs. open-path sensors on random errors across sites (Figure 9).

The total annual cumulative uncertainty in CH_4 fluxes, including both random and gap-filling errors, ranged from ± 0.01 to ± 13.4 g C m^{-2} y^{-1}, with a median value of ± 1.0 g C m^{-2} y^{-1} at 95% confidence (Figure 10a). Relative error decreased exponentially with flux magnitude, ranging from 1.5 % to 60% in most cases (Figure 10b), although a few sites where annual CH_4 sums were near zero had relative errors exceeding 200% (data not shown). The highest relative errors therefore tended to be associated with low CH_4-emitting sites, such as upland sites and bogs, and the lowest relative errors were generally associated with high CH_4-emitting sites such as freshwater marshes (Figure 10b).

Accepted for publication in *Bulletin of the American Meteorological Society.* DOI 10.1175/BAMS-D-18-0268.1.

5 Future research directions and needs

Better quantification of CH_4 sources and sinks will improve estimates of regional and global CH_4 budgets and reduce uncertainties in the CH_4 cycle. In this general context, high-frequency observations of ecosystem-scale CH_4 emissions should help constrain bottom-up CH_4 budgets, improve our understanding of the environmental factors controlling CH_4 fluxes, and inform and validate land-surface models used to estimate global CH_4 fluxes. Unlike well-established efforts synthesizing CO_2, water vapour, and energy observations, no such global data synthesis or initiative previously existed for CH_4. The database presented here addresses this gap with the EC community by organizing the collection and aggregation of a global EC CH_4 database through FLUXNET.

EC flux data quality assessment: Much of what has been learned within FLUXNET for CO_2, water vapour, and energy measurements is informing, and should continue to inform, new efforts for CH_4. Reliable EC measurements of CO_2 and water vapour fluxes have been conducted at hundreds of sites across broad regional networks (Papale et al. 2012), and substantial efforts have focused on developing best practices and harmonizing approaches across sites to ensure consistent, high-quality flux measurements (Aubinet et al. 1999; Reichstein et al. 2005; Moffat et al. 2007). CH_4 fluxes are often characterized by small fluxes with episodic spikes, and additional research is needed to ensure reliable measurements (Peltola et al. 2014, 2013), and refine and standardize methods and routines for data processing and quality checking (Nemitz et al. 2018; Schaller et al. 2018). Recent efforts provided guidance on instrument selection, setup and maintenance, and data processing for EC CH_4 flux measurements (Nemitz et al. 2018). However, with respect to instrument setup and data processing, more research is needed in best practices for storage flux quantification, despiking, and u_* filtering (Nemitz et al. 2018).

Accepted for publication in *Bulletin of the American Meteorological Society.* DOI 10.1175/BAMS-D-18-0268.1.

637 **Gap-filling**: Whereas neural networks have shown strong performance for gap-filling
638 CH_4 fluxes (Dengel et al. 2013; Knox et al. 2016), our results reveal some of the challenges of
639 gap-filling CH_4 fluxes at sites with low fluxes and/or a lack of seasonal and diel variation (Figure
640 8). More research is therefore needed for best practices for gap-filling to estimate annual CH_4
641 budgets (Nemitz et al. 2018). For example, there has yet to be a comprehensive analysis
642 comparing a wide range of gap-filling approaches for CH_4 fluxes similar to the study by Moffat
643 et al. (2007) for CO_2 exchange. While ANNs are one gap-filling method (Dengel et al. 2013;
644 Shoemaker et al. 2014; Morin et al. 2014a), numerous other gap-filling approaches exist,
645 including non-linear regression techniques, mean diurnal variation, look-up tables, marginal
646 distribution sampling, and the multiple imputation method (Moffat et al. 2007; Vitale et al.
647 2018). Future efforts should focus on systematically investigating these approaches across a
648 range of sites to provide best practices for gap-filling CH_4 exchange.
649 **Ancillary measurements**: Along with research that addresses the challenges of measuring
650 and processing EC CH_4 fluxes, key ancillary variables to help gap-fill, predict and scale CH_4
651 fluxes should also be measured more comprehensively across sites. For instance, although WTD
652 is known to strongly influence CH_4 emissions (Turetsky et al. 2014; Treat et al. 2018b), as noted
653 above, only half of the sites currently included in the database report water table position.
654 Generally, EC CH_4 measurements are implemented at sites also collecting CO_2 fluxes and
655 common meteorological measurements used in the flux community; however, guidelines are
656 only beginning to emerge for which additional supporting variables should be collected at sites
657 measuring CH_4 fluxes (Nemitz et al. 2018).
658 Measurements of variables beyond those relevant for CO_2 are needed to better understand
659 and predict the complex and interacting processes of CH_4 production, consumption and transport,

Accepted for publication in *Bulletin of the American Meteorological Society.* DOI 10.1175/BAMS-D-18-0268.1.

660 the latter of which includes diffusion, ebullition, and plant-mediated transport. Guidance on the
661 description of some basic variables affecting these processes is available through new protocols
662 in the flux community detailing soil meteorological measurements, ancillary vegetation
663 measurements, and site description, management and disturbance (Saunders et al. 2018; Op De
664 Beeck et al. 2018; Gielen et al. 2018). These protocols provide guidance on variables such as soil
665 temperature and soil moisture profiles, water table depth and snow depth, soil pH and soil type,
666 bulk density, and livestock density. However, although WTD is an easily measured proxy for
667 anaerobic conditions, direct and continuous measurement of redox potential and oxygen content
668 in particular would be valuable additional measurements (Nemitz et al. 2018). Similarly,
669 measuring variables such as conductivity, below-ground CH_4 concentrations, dissolved organic
670 carbon concentrations, and the presence of alternative electron acceptors such as nitrate, iron,
671 sulfate, and humic substances in the water and soil column would provide useful information for
672 the interpretation of CH_4 emissions. Stable isotope analyses of CH_4 are also valuable as they
673 provide important information on mechanisms of CH_4 production, transport, and oxidation
674 (Chanton et al. 1997; Marushchak et al. 2016). Detailed information on soil microbial
675 communities driving CH_4 production and consumption could also be helpful (Kwon et al. 2017).
676 Vegetation biomass, species composition and phenology are also important variables to consider,
677 because plants are a primary source of carbon substrates for methanogenic metabolism, and they
678 mediate CH_4 transport through aerenchymous tissue (Kwon et al. 2017; Joabsson et al. 1999;
679 Carmichael et al. 2014). New guidance is now available for such measurements at flux tower
680 locations (Gielen et al. 2018; Hufkens et al. 2018). Continuing to develop a consensus on best
681 practices for ancillary measurements is important for interpreting, gap-filling, and upscaling CH_4
682 flux measurements.

Accepted for publication in *Bulletin of the American Meteorological Society.* DOI 10.1175/BAMS-D-18-0268.1.

683 **Characterizing spatial variability**: CH_4 fluxes exhibit fine-scale spatial variability that can
684 span orders of magnitude within a landscape (Peltola et al. 2015; Marushchak et al. 2016; Desai
685 et al. 2015; Treat et al. 2018a; Iwata et al. 2018), attributable to heterogeneous soil properties and
686 moisture conditions, vegetation composition, and land-use (Davidson et al. 2016; Parmentier et
687 al. 2011; Chamberlain et al. 2018). Furthermore, there is evidence that traditionally unmeasured
688 surfaces (i.e., tree stems) are important sources of CH_4 to the atmosphere and could explain
689 spatial heterogeneity within ecosystems (Barba et al. 2019). Accurately representing spatial
690 heterogeneity and the relative fraction of uplands and wetlands is imperative for interpreting and
691 predicting CH_4 emissions within many ecosystems, and for upscaling flux measurements
692 regionally and globally as wetlands are hot spots for carbon cycling (Treat et al. 2018a; Tuovinen
693 et al. 2019; Rößger et al. 2019). Flux footprint analysis characterizing the fractional coverage of
694 the dominant surface types, particularly the fraction of open water and aerenchymatous plants, is
695 important for interpreting EC CH_4 flux measurements and quantifying annual CH_4 budgets at
696 spatially heterogeneous sites (Franz et al. 2016; Helbig et al. 2017a; Jammet et al. 2017) (Figure
697 11). This integration can be achieved by combining CH_4 measurements, flux footprint analysis,
698 and near-surface (e.g., phenocams) and/or high-resolution drone or satellite remote sensing data,
699 and should be common practice for all sites measuring CH_4 fluxes.
700 Spatial variability in ecosystem-scale CH_4 flux can further be examined by combining
701 chamber and EC measurements, including manual and auto-chambers, multi-tower approaches,
702 and airborne flux measurements (Peltola et al. 2015; Zona et al. 2016; Helbig et al. 2017a; Wolfe
703 et al. 2018; Kohnert et al. 2018; Lai et al. 2014; McNicol et al. 2017). Integrating additional
704 observations such as information on microbial communities, isotopic measurements, and
705 laboratory incubation observations along with chamber and EC CH_4 flux measurements can

Accepted for publication in *Bulletin of the American Meteorological Society.* DOI 10.1175/BAMS-D-18-0268.1.

further help explain CH_4 dynamics across scales (Angle et al. 2017; Chamberlain et al. 2018; Yang et al. 2017). However, as discussed above, additional research is needed to reconcile differences in fluxes measured across scales (Gioli et al. 2004; Holm et al. 2016; Meijide et al. 2011). Explicitly considering source area composition and spatial heterogeneity will provide enhanced processed-based understanding of CH_4 fluxes and improve upscaled regional and global estimates of CH_4 emissions, which can help reconcile the discrepancy between bottom-up and top-down budgets (Saunois et al. 2016a; Morin et al. 2017; Davidson et al. 2016).

More sites in key regions: We expect the number of flux towers measuring CH_4 fluxes will continue to grow (Chu et al. 2017; Pastorello et al. 2017; Morin 2018), but our compilation of EC CH_4 flux sites highlights key underrepresented regions where future flux towers are needed or where more efforts are needed for existing but non-reporting towers to contribute to FLUXNET (Figure 1). As noted previously, notable gaps include both tropical and subtropical regions, as well as eastern Canada, and the boreal forests of Russia. Figure 1 also provides guidance on where new towers could be strategically located to help reconcile differences between top-down and bottom-up estimates of wetland CH_4 emissions. In particular, substantial disagreements between top-down and bottom-up estimates are found over the Congo basin, the Inner Niger Delta, the Orinoco River Delta, the Maranon-Ucayali palm swamps, the Pantanal, the Ganges-Brahmaputra Delta, Sumatra, the western Siberian lowlands, and the Hudson Bay Lowlands (Figure 1). However, the placement of new towers is a strong function of the scientific question being asked and research funding priorities, and therefore the optimal tower network could be different for different applications (Mahecha et al. 2017; Papale et al. 2015; Villarreal et al. 2018).

Accepted for publication in *Bulletin of the American Meteorological Society.* DOI 10.1175/BAMS-D-18-0268.1.

Better understanding and representing processes: One of the biggest challenges for understanding ecosystem functioning is resolving overlapping, asynchronous (i.e., lagged) and nonlinear processes (Sturtevant et al. 2016). This challenge is particularly relevant for interpreting continuous, ecosystem-scale measurements of CH_4 exchange where scale-specific, nonlinear, and lagged processes may dominate (Franz *et al.*, 2016; Sturtevant *et al.*, 2016; Knox *et al.*, 2018). For instance, CH_4 emission responses to water table fluctuation can be nonlinear and lagged on the order of days to months (Goodrich *et al.*, 2015; Sturtevant *et al.*, 2016). CH_4 flux has also been observed to lag GPP by hours to days (Rinne et al. 2018; Hatala et al. 2012). Adequately representing these dynamics in process models is important, and further research is needed to better characterize the complex and nonlinear processes influencing ecosystem-scale CH_4 exchange across time scales.

The complex nature of CH_4 flux dynamics requires moving beyond traditional linear correlation and regression, and using methods such as wavelets, information theory, and Granger causality that are more tailored to address scale, nonlinearity, and lags directly (Stoy et al. 2005; Vargas et al. 2011; Schäfer et al. 2014; Knox et al. 2016; Detto et al. 2012). Through a USGS Powell Center working group activity, we will continue to investigate controls on CH_4 emissions within and across wetland types. To further explore interactions between ecosystem-scale CH_4 exchange and drivers across time scales, wavelet analysis will be combined with information theory to explore biosphere-atmosphere interactions regardless of form or asynchrony (Sturtevant et al. 2016; Knox et al. 2018; Chamberlain et al. 2018). By coupling wavelet decomposition with information theory, future research will investigate key controls on CH_4 fluxes across time scales, as well as the importance of nonlinearities and lags in predicting CH_4 flux dynamics. Future research will also use the global CH_4 database to parameterize and

Accepted for publication in *Bulletin of the American Meteorological Society.* DOI 10.1175/BAMS-D-18-0268.1.

benchmark the performance of land-surface models of global CH_4 emissions, providing a unique opportunity for informing and validating biogeochemical models.

Coordinating, organizing and improving the integration of CH_4 fluxes in regional networks and ultimately FLUXNET will bring us one step closer to achieving the goal of providing flux information "everywhere and all of the time" (Baldocchi 2008). In the long-term, we hope to integrate the global eddy covariance CH_4 database with other methods for measuring CH_4 fluxes, such as chamber, aircraft, and satellite measurements. By integrating CH_4 flux measurements, remote sensing, and modeling, we aim to better characterize CH_4 emissions from terrestrial ecosystems and ultimately reduce uncertainties in the global CH_4 cycle.

Acknowledgments

This study was supported by the Gordon and Betty Moore Foundation through Grant GBMF5439 "Advancing Understanding of the Global Methane Cycle" to Stanford University supporting the Methane Budget activity for the Global Carbon Project (globalcarbonproject.org). This work was also conducted as a part of the Wetland FLUXNET Synthesis for Methane Working Group supported by the John Wesley Powell Center for Analysis and Synthesis of the U.S. Geological Survey. We acknowledge the following AmeriFlux sites for their data records: CA-SCC, CA-SCB, US-Beo, US-Bes, US-Atq, US-Ivo, US-ICs, US-NGB, US-NGC, US-Los, US-NC4, US-HRA, US-HRC, US-Myb, US-Sne, US-Tw1, US-Tw4, US-Twt, US-Bi2, US-Bi1, US-Snd, US-OWC, US-ORv, US-WPT, US-CRT, US-MRM, US-Srr, US-Uaf, US-Ho1, US-StJ, US-LA2, US-LA1. In addition, funding for AmeriFlux data resources were provided by the U.S. Department of Energy's Office of Science. BRKR was supported by NSF Award 1752083. TFK and HC acknowledge support from the

Accepted for publication in *Bulletin of the American Meteorological Society.* DOI 10.1175/BAMS-D-18-0268.1.

AmeriFlux Management Project. Any use of trade, firm, or product names is for descriptive purposes only and does not imply endorsement by the U.S. Government. DP, IM and TV thank the EU for supporting the RINGO project funded by the Horizon 2020 Research and Innovation Programme under grant agreement 730944.

Accepted for publication in *Bulletin of the American Meteorological Society.* DOI 10.1175/BAMS-D-18-0268.1.

780 **Appendix A: Sites currently included in the database**

781 **Table A1** here

782

Accepted for publication in *Bulletin of the American Meteorological Society.* DOI 10.1175/BAMS-D-18-0268.1.

References

Anderson, D. E., S. B. Verma, and N. J. Rosenberg, 1984: Eddy correlation measurements of CO2, latent heat, and sensible heat fluxes over a crop surface. *Boundary-Layer Meteorol.*, **29**, 263–272, doi:10.1007/BF00119792.

Anderson, F. E., and Coauthors, 2016: Variation of energy and carbon fluxes from a restored temperate freshwater wetland and implications for carbon market verification protocols. *J. Geophys. Res. Biogeosciences*, **121**, 777–795, doi:10.1002/2015JG003083.

Angle, J. C., and Coauthors, 2017: Methanogenesis in oxygenated soils is a substantial fraction of wetland methane emissions. *Nat. Commun.*, **8**, 1567, doi:10.1038/s41467-017-01753-4.

Arcus, V. L., E. J. Prentice, J. K. Hobbs, A. J. Mulholland, M. W. Van Der Kamp, C. R. Pudney, E. J. Parker, and L. A. Schipper, 2016: On the Temperature Dependence of Enzyme-Catalyzed Rates. *Biochemistry*, **55**, 1681–1688, doi:10.1021/acs.biochem.5b01094.

Aubinet, M., and Coauthors, 1999: Estimates of the annual net carbon and water exchange of forests: The EUROFLUX methodology. *Adv. Ecol. Res.*, **30**, 113–175, doi:10.1016/S0065-2504(08)60018-5.

Aubinet, M., T. Vesala, and D. Papale, 2012: *Eddy Covariance - A Practical Guide to Measurement and Data Analysis*. Springer,.

Baldocchi, D. D., 2003: Assessing the eddy covariance technique for evaluating carbon dioxide exchange rates of ecosystems: past, present and future. *Glob. Chang. Biol.*, **9**, 479–492, doi:10.1046/j.1365-2486.2003.00629.x.

——, 2008: 'Breathing' of the terrestrial biosphere: lessons learned from a global network of carbon dioxide flux measurement systems. *Aust. J. Bot.*, **56**, 1–26, doi:10.1071/BT07151.

——, 2014: Measuring fluxes of trace gases and energy between ecosystems and the atmosphere

Accepted for publication in *Bulletin of the American Meteorological Society.* DOI 10.1175/BAMS-D-18-0268.1.

– the state and future of the eddy covariance method. *Glob. Chang. Biol.*, **20**, 3600–3609, doi:10.1111/gcb.12649.

Barba, J., and Coauthors, 2019: Methane emissions from tree stems: a new frontier in the global carbon cycle. *New Phytol.*, **222**, 18–28, doi:10.1111/nph.15582.

Bartlett, K. B., and R. C. Harriss, 1993: Review and assessment of methane emissions from wetlands. **26**, 261–320.

Bastviken, D., L. J. Tranvik, J. A. Downing, P. M. Crill, and A. Enrich-Prast, 2011: Freshwater methane emissions offset the continental carbon sink. *Science*, **331**, 50, doi:10.1126/science.1196808.

Bates, D., M. Mächler, B. Bolker, and S. Walker, 2014: Fitting linear mixed-effects models using lme4. **67**, doi:10.18637/jss.v067.i01.

——, M. Machler, B. Bolker, and S. Walker, 2015: *Fitting linear mixed-effects models using lme4*. vol. 67, p. 48. pp.

Op De Beeck, M., and Coauthors, 2018: Soil-meteorological measurements at ICOS monitoring stations in terrestrial ecosystems. *Int. Agrophys*, **32**, 619–631, doi:10.1515/intag-2017-0041.

Bousquet, P., and Coauthors, 2006: Contribution of anthropogenic and natural sources to atmospheric methane variability. *Nature*, **443**, 439–443, doi:10.1038/nature05132.

Bridgham, S. D., H. Cadillo-Quiroz, J. K. Keller, and Q. Zhuang, 2013: Methane emissions from wetlands: Biogeochemical, microbial, and modeling perspectives from local to global scales. *Glob. Chang. Biol.*, **19**, 1325–1346, doi:10.1111/gcb.12131.

Brix, H., B. K. Sorrell, and P. T. Orr, 1992: Internal pressurization and convective gas flow in some emergent freshwater macrophytes. *Limnol. Oceanogr.*, **37**, 1420–1433, doi:10.4319/lo.1992.37.7.1420.

Accepted for publication in *Bulletin of the American Meteorological Society.* DOI 10.1175/BAMS-D-18-0268.1.

829 Bubier, J., T. Moore, K. Savage, and P. Crill, 2005: A comparison of methane flux in a boreal
830 landscape between a dry and a wet year. *Global Biogeochem. Cycles*, **19**,
831 doi:10.1029/2004GB002351.
832 Carmichael, M. J., E. S. Bernhardt, S. L. Bräuer, and W. K. Smith, 2014: The role of vegetation
833 in methane flux to the atmosphere: should vegetation be included as a distinct category in
834 the global methane budget? *Biogeochemistry*, **119**, 1–24, doi:10.1007/s10533-014-9974-1.
835 Castro-Morales, K., T. Kleinen, S. Kaiser, S. Zaehle, F. Kit-Tler, M. J. Kwon, C. Beer, and M.
836 Göckede, Year-round simulated methane emissions from a permafrost ecosystem in
837 Northeast Siberia. doi:10.5194/bg-2017-310.
838 Cazelles, B., M. Chavez, D. Berteaux, F. Ménard, J. O. Vik, S. Jenouvrier, and N. C. Stenseth,
839 2008: Wavelet analysis of ecological time series. *Oecologia*, **156**, 287–304,
840 doi:10.1007/s00442-008-0993-2.
841 Chamberlain, S. D., and Coauthors, 2018: Soil properties and sediment accretion modulate
842 methane fluxes from restored wetlands. *Glob. Chang. Biol.*, **24**, 4107–4121,
843 doi:10.1111/gcb.14124.
844 Chanton, J. P., G. J. Whiting, J. D. Happell, and G. Gerard, 1993: Contrasting rates and diurnal
845 patterns of methane emission from emergent aquatic macrophytes. *Aquat. Bot.*, **46**, 111–
846 128, doi:http://dx.doi.org/10.1016/0304-3770(93)90040-4.
847 Chanton, J. P., G. J. Whiting, N. E. Blair, C. W. Lindau, and P. K. Bollich, 1997: Methane
848 emission from rice: Stable isotopes, dirunal variations, and CO2 exchange. *Global*
849 *Biogeochem. Cycles*, **11**, 15–27.
850 Chen, Y.-H., and R. G. Prinn, 2006: Estimation of atmospheric methane emissions between 1996
851 and 2001 using a three-dimensional global chemical transport model. *J. Geophys. Res.*

Accepted for publication in *Bulletin of the American Meteorological Society.* DOI 10.1175/BAMS-D-18-0268.1.

Atmos., **111**, doi:10.1029/2005JD006058.

Christensen, T. R., and Coauthors, 2003: Factors controlling large scale variations in methane emissions from wetlands. *Geophys. Res. Lett.*, **30**, doi:10.1029/2002GL016848.

Chu, H., J. Chen, J. F. Gottgens, Z. Ouyang, R. John, K. Czajkowski, and R. Becker, 2014: Net ecosystem methane and carbon dioxide exchanges in a Lake Erie coastal marsh and a nearby cropland. *J. Geophys. Res. Biogeosciences*, **119**, 722–740, doi:10.1002/2013JG002520.

——, D. D. Baldocchi, R. John, S. Wolf, and M. Reichstein, 2017: Fluxes all of the time? A primer on the temporal representativeness of FLUXNET. *J. Geophys. Res. Biogeosciences*, **122**, 289–307, doi:10.1002/2016JG003576.

Davidson, S. J., V. L. Sloan, G. K. Phoenix, R. Wagner, J. P. Fisher, W. C. Oechel, and D. Zona, 2016: Vegetation Type Dominates the Spatial Variability in CH4 Emissions Across Multiple Arctic Tundra Landscapes. *Ecosystems*, **19**, 1116–1132, doi:10.1007/s10021-016-9991-0.

Dean, J. F., and Coauthors, 2018: Methane feedbacks to the global climate system in a warmer world. *Rev. Geophys.*, 1–44, doi:10.1002/2017RG000559.

Dengel, S., D. Zona, T. Sachs, M. Aurela, M. Jammet, F. J. W. Parmentier, W. Oechel, and T. Vesala, 2013: Testing the applicability of neural networks as a gap-filling method using CH4 flux data from high latitude wetlands. *Biogeosciences*, **10**, 8185–8200, doi:10.5194/bg-10-8185-2013.

Desai, A. R., and Coauthors, 2015: Landscape-level terrestrial methane flux observed from a very tall tower. *Agric. For. Meteorol.*, **201**, 61–75, doi:10.1016/j.agrformet.2014.10.017.

Desjardins, R. L., 1974: A technique to measure CO2 exchange under field conditions. *Int. J.*

Accepted for publication in *Bulletin of the American Meteorological Society.* DOI 10.1175/BAMS-D-18-0268.1.

Biometeorol., **18**, 76–83, doi:10.1007/BF01450667.

Detto, M., A. Molini, G. Katul, P. Stoy, S. Palmroth, and D. Baldocchi, 2012: Causality and persistence in ecological systems: A nonparametric spectral Granger Causality approach. *Source Am. Nat.*, **179**, 21, doi:10.1086/664628.

Euskirchen, E. S., M. S. Bret-Harte, G. R. Shaver, C. W. Edgar, and V. E. Romanovsky, 2017: Long-term release of carbon dioxide from arctic tundra ecosystems in Alaska. *Ecosystems*, **20**, doi:10.1007/s10021-016-0085-9.

Fan, S. M., and Coauthors, 1992: Micrometeorological measurements of CH4 and CO2 exchange between the atmosphere and subarctic tundra. *J. Geophys. Res.*, **97**, 16627, doi:10.1029/91JD02531.

Franz, D., F. Koebsch, E. Larmanou, J. Augustin, and T. Sachs, 2016: High net CO2 and CH4 release at a eutrophic shallow lake on a formerly drained fen. *Biogeosciences*, **13**, 3051–3070, doi:10.5194/bg-13-3051-2016.

Gielen, B., and Coauthors, 2018: Ancillary vegetation measurements at ICOS ecosystem stations. *Sara Marañon-Jimenez*, **10**, 645–664, doi:10.1515/intag-2017-0048.

Gioli, B., and Coauthors, 2004: Comparison between tower and aircraft-based eddy covariance fluxes in five European regions. *Agric. For. Meteorol.*, **127**, 1–16, doi:10.1016/j.agrformet.2004.08.004.

Goodrich, J. P., D. I. Campbell, N. T. Roulet, M. J. Clearwater, and L. A. Schipper, 2015: Overriding control of methane flux temporal variability by water table dynamics in a Southern Hemisphere, raised bog. *J. Geophys. Res. Biogeosciences*, **120**, 819–831, doi:10.1002/2014JG002844.Received.

Grant, R. F., and N. T. Roulet, 2002: Methane efflux from boreal wetlands: Theory and testing of

Accepted for publication in *Bulletin of the American Meteorological Society.* DOI 10.1175/BAMS-D-18-0268.1.

the ecosystem model Ecosys with chamber and tower flux measurements. *Global Biogeochem. Cycles*, **16**, 2-1-2–16, doi:10.1029/2001GB001702.

Harris, I., P. D. Jones, T. J. Osborn, and D. H. Lister, 2014: Updated high-resolution grids of monthly climatic observations - the CRU TS3.10 Dataset. *Int. J. Climatol.*, **34**, 623–642, doi:10.1002/joc.3711.

Hatala, J. A., M. Detto, and D. D. Baldocchi, 2012: Gross ecosystem photosynthesis causes a diurnal pattern in methane emission from rice. *Geophys. Res. Lett.*, **39**, 1–5, doi:10.1029/2012GL051303.

Helbig, M., L. E. Chasmer, N. C. Kljun, W. L. Quinton, C. C. Treat, and O. Sonnentag, 2017a: The positive net radiative greenhouse gas forcing of increasing methane emissions from a thawing boreal forest-wetland landscape. *Glob. Chang. Biol.*, **23**, 2413–2427, doi:10.1111/gcb.13520.

——, W. L. Quinton, and O. Sonnentag, 2017b: Warmer spring conditions increase annual methane emissions from a boreal peat landscape with sporadic permafrost. *Environ. Res. Lett.*, **12**, 115009, doi:10.1088/1748-9326/aa8c85.

Hendriks, D. M. D., J. van Huissteden, and A. J. Dolman, 2010: Multi-technique assessment of spatial and temporal variability of methane fluxes in a peat meadow. *Agric. For. Meteorol.*, **150**, 757–774, doi:10.1016/J.AGRFORMET.2009.06.017.

Hollinger, A. D., and A. D. Richardson, 2005: Uncertainty in eddy covariance measurements and its application to physiological models. *Tree Physiol.*, **25**, 873–885, doi:10.1093/treephys/25.7.873.

Holm, G. O., B. C. Perez, D. E. McWhorter, K. W. Krauss, D. J. Johnson, R. C. Raynie, and C. J. Killebrew, 2016: Ecosystem level methane fluxes from tidal freshwater and brackish

Accepted for publication in *Bulletin of the American Meteorological Society.* DOI 10.1175/BAMS-D-18-0268.1.

marshes of the ississippi River Delta: Implications for coastal wetland carbon projects. *Wetlands*, **36**, 401–413, doi:10.1007/s13157-016-0746-7.

Hufkens, K., and Coauthors, 2018: Assimilating phenology datasets automatically across ICOS ecosystem stations. *Int. Agrophys*, **32**, 677–687, doi:10.1515/intag-2017-0050.

Iwata, H., R. Hirata, Y. Takahashi, Y. Miyabara, M. Itoh, and K. Iizuka, 2018: Partitioning eddy-covariance methane fluxes from a shallow lake into diffusive and ebullitive Fluxes. *Boundary-Layer Meteorol.*, **169**, 413–428, doi:10.1007/s10546-018-0383-1.

Jackowicz-Korczyński, M., T. R. Christensen, K. Bäckstrand, P. Crill, T. Friborg, M. Mastepanov, and L. Ström, 2010: Annual cycle of methane emission from a subarctic peatland. *J. Geophys. Res. G Biogeosciences*, **115**, 1–10, doi:10.1029/2008JG000913.

Jammet, M., S. Dengel, E. Kettner, F.-J. W. Parmentier, M. Wik, P. Crill, and T. Friborg, 2017: Year-round CH4 and CO2 flux dynamics in two contrasting freshwater ecosystems of the subarctic. *Biogeosciences*, **145194**, 5189–5216, doi:10.5194/bg-14-5189-2017.

Joabsson, A., T. R. Christensen, and B. Wallén, 1999: Vascular plant controls on methane emissions from northern peatforming wetlands. *Trends Ecol. Evol.*, **14**, 385–388, doi:10.1016/S0169-5347(99)01649-3.

Jung, M., M. Reichstein, and A. Bondeau, 2009: Towards global empirical upscaling of FLUXNET eddy covariance observations: Validation of a model tree ensemble approach using a biosphere model. *Biogeosciences*, **6**, 2001–2013, doi:10.5194/bg-6-2001-2009.

Kim, J., S. B. Verma, and D. P. Billesbach, 1999: Seasonal variation in methane emission from a temperate Phragmites-dominated marsh: effect of growth stage and plant-mediated transport. *Glob. Chang. Biol.*, **5**, 433–440, doi:10.1046/j.1365-2486.1999.00237.x.

Kittler, F., M. Heimann, O. Kolle, N. Zimov, S. Zimov, and M. Göckede, 2017: Long-Term

Accepted for publication in *Bulletin of the American Meteorological Society.* DOI 10.1175/BAMS-D-18-0268.1.

Drainage Reduces CO2 Uptake and CH4 Emissions in a Siberian Permafrost Ecosystem. *Global Biogeochem. Cycles*, **31**, 1704–1717, doi:10.1002/2017GB005774.

Kljun, N., P. Calanca, M. W. Rotach, and H. P. Schmid, 2015: A simple two-dimensional parameterisation for Flux Footprint Prediction (FFP). *Geosci. Model Dev*, **8**, 3695–3713, doi:10.5194/gmd-8-3695-2015.

Knox, S. H., C. Sturtevant, J. H. Matthes, L. Koteen, J. Verfaillie, and D. Baldocchi, 2015: Agricultural peatland restoration: Effects of land-use change on greenhouse gas (CO2 and CH4) fluxes in the Sacramento-San Joaquin Delta. *Glob. Chang. Biol.*, **21**, 750–765, doi:10.1111/gcb.12745.

——, J. H. Matthes, C. Sturtevant, P. Y. Oikawa, J. Verfaillie, and D. Baldocchi, 2016: Biophysical controls on interannual variability in ecosystem-scale CO2 and CH4 exchange in a California rice paddy. *J. Geophys. Res. Biogeosciences*, **121**, 978–1001, doi:10.1002/2015JG003247.Received.

——, L. Windham-Myers, F. Anderson, C. Sturtevant, and B. Bergamaschi, 2018: Direct and Indirect Effects of Tides on Ecosystem-Scale CO2Exchange in a Brackish Tidal Marsh in Northern California. *J. Geophys. Res. Biogeosciences*, **123**, 787–806, doi:10.1002/2017JG004048.

Koebsch, F., G. Jurasinski, M. Koch, J. Hofmann, and S. Glatzel, 2015: Controls for multi-scale temporal variation in ecosystem methane exchange during the growing season of a permanently inundated fen. *Agric. For. Meteorol.*, **204**, 94–105, doi:10.1016/J.AGRFORMET.2015.02.002.

Kohnert, K., B. Juhls, S. Muster, S. Antonova, A. Serafimovich, S. Metzger, J. Hartmann, and T. Sachs, 2018: Toward understanding the contribution of waterbodies to the methane

Accepted for publication in *Bulletin of the American Meteorological Society.* DOI 10.1175/BAMS-D-18-0268.1.

emissions of a permafrost landscape on a regional scale-A case study from the Mackenzie Delta, Canada. *Glob. Chang. Biol.*, **24**, 3976–3989, doi:10.1111/gcb.14289.

Kormann, R., and F. X. Meixner, 2001: An analytical footprint model for non-neutral stratification. *Boundary-Layer Meteorol.*, **99**, 207–224, doi:10.1023/A:1018991015119.

Krauss, K. W., and Coauthors, 2016: Component greenhouse gas fluxes and radiative balance from two deltaic marshes in Louisiana: Pairing chamber techniques and eddy covariance. *J. Geophys. Res. Biogeosciences*, **121**, 1503–1521, doi:10.1002/2015JG003224.

Kwon, M. J., and Coauthors, 2017: Plants, microorganisms, and soil temperatures contribute to a decrease in methane fluxes on a drained Arctic floodplain. *Glob. Chang. Biol.*, **23**, 2396–2412, doi:10.1111/gcb.13558.

Lai, D. Y. F., T. R. Moore, and N. T. Roulet, 2014: Spatial and temporal variations of methane flux measured by autochambers in a temperate ombrotrophic peatland. *J. Geophys. Res. Biogeosciences*, **119**, 864–880, doi:10.1002/2013JG002410.

Lasslop, G., M. Reichsten, D. Papale, A. D. RIichardson, A. Arneth, A. Barr, P. Stoy, and G. Wohlfahrt, 2010: Separation of net ecosystem exchange into assimilation and respiration using a light response curve approach: critical issues and global evaluation. *Glob. Chang. Biol.*, **16**, 187–208, doi:10.1111/j.1365-2486.2009.02041.x.

Lehner, B., and P. Döll, 2004: Development and validation of a global database of lakes, reservoirs and wetlands. *J. Hydrol.*, **296**, 1–22, doi:10.1016/J.JHYDROL.2004.03.028.

Mahecha, M. D., and Coauthors, 2017: Detecting impacts of extreme events with ecological in situ monitoring networks. *Biogeosciences*, **14**, 4255–4277, doi:10.5194/bg-14-4255-2017.

Marushchak, M. E., and Coauthors, 2016: Methane dynamics in the subarctic tundra: Combining stable isotope analyses, plot-And ecosystem-scale flux measurements. *Biogeosciences*, **13**,

Accepted for publication in *Bulletin of the American Meteorological Society.* DOI 10.1175/BAMS-D-18-0268.1.

597–608, doi:10.5194/bg-13-597-2016.

McDermitt, D., and Coauthors, 2011: A new low-power, open-path instrument for measuring methane flux by eddy covariance. *Appl. Phys. B*, **102**, 391–405, doi:10.1007/s00340-010-4307-0.

McNicol, G., C. S. Sturtevant, S. H. Knox, I. Dronova, D. D. Baldocchi, and W. L. Silver, 2017: Effects of seasonality, transport pathway, and spatial structure on greenhouse gas fluxes in a restored wetland. *Glob. Chang. Biol.*, n/a-n/a, doi:10.1111/gcb.13580.

McNorton, J., and Coauthors, 2016: Role of regional wetland emissions in atmospheric methane variability. *Geophys. Res. Lett.*, **43**, 11,433-11,444, doi:10.1002/2016GL070649.

Meijide, A., G. Manca, I. Goded, V. Magliulo, P. di Tommasi, G. Seufert, and A. Cescatti, 2011: Seasonal trends and environmental controls of methane emissions in a rice paddy field in Northern Italy. *Biogeosciences*, **8**, 3809–3821, doi:10.5194/bg-8-3809-2011.

Melton, J. R., and Coauthors, 2013: Geoscientific Instrumentation Methods and Data Systems Present state of global wetland extent and wetland methane modelling: conclusions from a model inter-comparison project (WETCHIMP). *Biogeosciences*, **10**, 753–788, doi:10.5194/bg-10-753-2013.

Mitsch, W. J., A. Nahlik, P. Wolski, B. Bernal, L. Zhang, and L. Ramberg, 2009: Tropical wetlands: seasonal hydrologic pulsing, carbon sequestration, and methane emissions. doi:10.1007/s11273-009-9164-4.

Moffat, A. M., and Coauthors, 2007: Comprehensive comparison of gap-filling techniques for eddy covariance net carbon fluxes. *Agric. For. Meteorol.*, **147**, 209–232, doi:10.1016/j.agrformet.2007.08.011.

Morin, T. H., 2018: Advances in the eddy covariance approach to CH4 monitoring over two and

Accepted for publication in *Bulletin of the American Meteorological Society.* DOI 10.1175/BAMS-D-18-0268.1.

a half decades. *J. Geophys. Res. Biogeosciences*, doi:10.1029/2018JG004796.

——, G. Bohrer, R. P. d. M. Frasson, L. Naor-Azreli, S. Mesi, K. C. Stefanik, and K. V. R. Schäfer, 2014a: Environmental drivers of methane fluxes from an urban temperate wetland park. *J. Geophys. Res. Biogeosciences*, **119**, 2188–2208, doi:10.1002/2014JG002750.

——, ——, L. Naor-Azrieli, S. Mesi, W. T. Kenny, W. J. Mitsch, and K. V. R. Schäfer, 2014b: The seasonal and diurnal dynamics of methane flux at a created urban wetland. *Ecol. Eng.*, **72**, 74–83, doi:10.1016/j.ecoleng.2014.02.002.

——, ——, K. C. Stefanik, A. C. Rey-Sanchez, A. M. Matheny, and W. J. Mitsch, 2017: Combining eddy-covariance and chamber measurements to determine the methane budget from a small, heterogeneous urban floodplain wetland park. *Agric. For. Meteorol.*, **237**–**238**, 160–170, doi:10.1016/J.AGRFORMET.2017.01.022.

Myhre, G., and Coauthors, 2013: Anthropogenic and natural radiative forcing. *Climate Change 2013: The Physical Science Basis. Contribution of Working Group I to the Fifth Assessment Report of the Intergovernmental Panel on Climate Change*, T.F. Stocker et al., Eds., Cambridge University Press, Cambridge, United Kingdom and New York, NY, USA, 659–740.

Nadeau, D. F., A. N. Rousseau, C. Coursolle, H. A. Margolis, and M. B. Parlange, 2013: Summer methane fluxes from a boreal bog in northern Quebec, Canada, using eddy covariance measurements. doi:10.1016/j.atmosenv.2013.09.044.

Nakagawa, S., and H. Schielzeth, 2013: A general and simple method for obtaining R2 from generalized linear mixed-effects models. *Methods Ecol. Evol.*, **4**, 133–142, doi:10.1111/j.2041-210x.2012.00261.x.

Nemitz, E., and Coauthors, 2018: Standardisation of eddy-covariance flux measurements of

Accepted for publication in *Bulletin of the American Meteorological Society.* DOI 10.1175/BAMS-D-18-0268.1.

methane and nitrous oxide. *Int. Agrophys*, **32**, 517–549, doi:10.1515/intag-2017-0042.

Oikawa, P. Y., and Coauthors, 2017: Evaluation of a hierarchy of models reveals importance of substrate limitation for predicting carbon dioxide and methane exchange in restored wetlands. *J. Geophys. Res. Biogeosciences*, **122**, 145–167, doi:10.1002/2016JG003438.

Olefeldt, D., M. R. Turetsky, P. M. Crill, and A. D. McGuire, 2013: Environmental and physical controls on northern terrestrial methane emissions across permafrost zones. *Glob. Chang. Biol.*, **19**, 589–603, doi:10.1111/gcb.12071.

Olson, D. M., and Coauthors, 2001: Terrestrial ecoregions of the world: A new map of life on Earth. *Bioscience*, **51**, 933–938, doi:10.1641/0006-3568(2001)051[0933:TEOTWA]2.0.CO;2.

Pangala, S. R., and Coauthors, 2017: Large emissions from floodplain trees close the Amazon methane budget. *Nature*, **552**, 230–234, doi:10.1038/nature24639.

Papale, D., D. Agarwal, D. Baldocchi, R. Cook, J. B. Fisher, and C. van Ingen, 2012: Database maintenance, data sharing policy, collaboration. *Eddy Covariance: A Practical Guide to Measurement and Data Analysis*, M. Aubinet, T. Vesala, and D. Papale, Eds., Springer Science+Business Media B.V, Netherlands, 399–424.

——, and Coauthors, 2015: Effect of spatial sampling from European flux towers for estimating carbon and water fluxes with artificial neural networks. *J. Geophys. Res. Biogeosciences*, **120**, 1941–1957, doi:10.1002/2015JG002997.

Parmentier, F. J. W., J. Van Huissteden, M. K. Van Der Molen, G. Schaepman-Strub, S. A. Karsanaev, T. C. Maximov, and A. J. Dolman, 2011: Spatial and temporal dynamics in eddy covariance observations of methane fluxes at a tundra site in northeastern Siberia. *J. Geophys. Res. Biogeosciences*, **116**, 1–14, doi:10.1029/2010JG001637.

Accepted for publication in *Bulletin of the American Meteorological Society.* DOI 10.1175/BAMS-D-18-0268.1.

Pastorello, G. Z., D. Papale, H. Chu, C. Trotta, D. Agarwal, E. Canfora, D. Baldocchi, and M. Torn, 2017: A new data set to keep a sharper eye on land-air exchanges. *Eos (Washington. DC).*, **98**, doi:10.1029/2017EO071597.

Peltola, O., I. Mammarella, S. Haapanala, G. Burba, and T. Vesala, 2013: Climate of the Past Geoscientific Instrumentation Methods and Data Systems Field intercomparison of four methane gas analyzers suitable for eddy covariance flux measurements. *Biogeosciences,* **10**, 3749–3765, doi:10.5194/bg-10-3749-2013.

——, and Coauthors, 2014: Evaluating the performance of commonly used gas analysers for methane eddy covariance flux measurements: the InGOS inter-comparison field experiment. *Biogeosciences,* **11**, 3163–3186, doi:10.5194/bg-11-3163-2014.

——, and Coauthors, 2015: Studying the spatial variability of methane flux with five eddy covariance towers of varying height. *Agric. For. Meteorol.*, **214**–**215**, 456–472, doi:10.1016/j.agrformet.2015.09.007.

——, and Coauthors, 2019: Monthly Gridded Data Product of Northern Wetland Methane Emissions Based on Upscaling Eddy Covariance Observations. *Earth Syst. Sci. Data*, **Discussion**, doi:10.5194/essd-2019-28.

Petrescu, A. M. R., and Coauthors, 2015: The uncertain climate footprint of wetlands under human pressure. *Proc. Natl. Acad. Sci.*, **112**, 4594–4599, doi:10.1073/pnas.1416267112.

Poffenbarger, H., B. Needelman, and J. P. Megonigal, 2011: Salinity influence on methane emissions from tidal marshes. *Wetlands,* **31**, 831–842, doi:10.1007/s13157-011-0197-0.

Poulter, B., and Coauthors, 2017: Global wetland contribution to 2000–2012 atmospheric methane growth rate dynamics. *Environ. Res. Lett.*, **12**, 094013, doi:10.1088/1748-9326/aa8391.

Accepted for publication in *Bulletin of the American Meteorological Society.* DOI 10.1175/BAMS-D-18-0268.1.

1082 Pugh, C. A., D. E. Reed, A. R. Desai, and B. N. Sulman, 2018: Wetland flux controls: how does
1083 interacting water table levels and temperature influence carbon dioxide and methane fluxes
1084 in northern Wisconsin? *Biogeochemistry*, **137**, 15–25, doi:10.1007/s10533-017-0414-x.
1085 Reichstein, M., and Coauthors, 2005: On the separation of net ecosystem exchange into
1086 assimilation and ecosystem respiration: review and improved algorithm. *Glob. Chang. Biol.*,
1087 **11**, 1424–1439, doi:10.1111/j.1365-2486.2005.001002.x.
1088 Rey-Sanchez, A. C., T. H. Morin, K. C. Stefanik, K. Wrighton, and G. Bohrer, 2018:
1089 Determining total emissions and environmental drivers of methane flux in a Lake Erie
1090 estuarine marsh. *Ecol. Eng.*, **114**, 7–15, doi:10.1016/J.ECOLENG.2017.06.042.
1091 Richardson, A. D., and D. Y. Hollinger, 2007: A method to estimate the additional uncertainty in
1092 gap-filled NEE resulting from long gaps in the CO2 flux record. *Agric. For. Meteorol.*, **147**,
1093 199–208, doi:10.1016/j.agrformet.2007.06.004.
1094 ——, and Coauthors, 2006: A multi-site analysis of random error in tower-based measurements
1095 of carbon and energy fluxes. *Agric. For. Meteorol.*, **136**, 1–18,
1096 doi:http://dx.doi.org/10.1016/j.agrformet.2006.01.007.
1097 ——, and Coauthors, 2008: Statistical properties of random CO2 flux measurement uncertainty
1098 inferred from model residuals. *Agric. For. Meteorol.*, **148**, 38–50,
1099 doi:10.1016/J.AGRFORMET.2007.09.001.
1100 ——, M. Aubinet, A. G. Barr, D. Y. Hollinger, A. Ibrom, G. Lasslop, and M. Reichstein, 2012:
1101 Uncertainty Quantification. *Eddy Covariance: A Practical Guide to Measurement and Data*
1102 *Analysis*, M. Aubinet, T. Vesala, and D. Papale, Eds., Springer Netherlands, Dordrecht,
1103 173–209.
1104 Riley, W. J., Z. M. Subin, D. M. Lawrence, S. C. Swenson, M. S. Torn, L. Meng, N. M.

Accepted for publication in *Bulletin of the American Meteorological Society.* DOI 10.1175/BAMS-D-18-0268.1.

Mahowald, and P. Hess, 2011: Barriers to predicting changes in global terrestrial methane fluxes: analyses using CLM4Me, a methane biogeochemistry model integrated in CESM. *Biogeosciences*, **8**, 1925–1953, doi:10.5194/bg-8-1925-2011.

Rinne, J., T. Riutta, M. Pihlatie, M. Aurela, S. Haapanala, J.-P. Tuovinen, E.-S. Tuittila, and T. Vesala, 2007: Annual cycle of methane emission from a boreal fen measured by the eddy covariance technique. *Tellus B Chem. Phys. Meteorol.*, **59**, 449–457, doi:10.1111/j.1600-0889.2007.00261.x.

——, and Coauthors, 2018: Temporal variation of ecosystem scale methane emission from a boreal fen in relation to temperature, water table position, and carbon dioxide fluxes. *Global Biogeochem. Cycles*, **32**, 1087–1106, doi:10.1029/2017GB005747.

Rößger, N., C. Wille, G. Veh, J. Boike, and L. Kutzbach, 2019: Scaling and balancing methane fluxes in a heterogeneous tundra ecosystem of the Lena River Delta. *Agric. For. Meteorol.*, **266**–**267**, 243–255, doi:10.1016/J.AGRFORMET.2018.06.026.

Runkle, B. R. K., K. Suvoč, M. L. Reba, C. W. Reavis, S. F. Smith, Y.-L. Chiu, and B. Fong, 2019: Methane Emission Reductions from the Alternate Wetting and Drying of Rice Fields Detected Using the Eddy Covariance Method. *Environ. Sci. Technol.*, **53**, 671–681, doi:10.1021/acs.est.8b05535.

Sachs, T., C. Wille, J. Boike, and L. Kutzbach, 2008: Environmental controls on ecosystem-scale CH4 emission from polygonal tundra in the Lena River Delta, Siberia. *J. Geophys. Res*, **113**, 0–3, doi:10.1029/2007JG000505.

Sass, R., 2003: CH4 emissions from rice agriculture. *IPCC Expert Meet. Good Pract. Guid. Uncertain. Manag. Natl. Greenh. Gas Invent.*, 399–417.

Saunders, M., and Coauthors, 2018: Importance of reporting ancillary site characteristics, and

Accepted for publication in *Bulletin of the American Meteorological Society.* DOI 10.1175/BAMS-D-18-0268.1.

management and disturbance information at ICOS stations. *Int. Agrophys*, **32**, 457–469, doi:10.1515/intag-2017-0040.

Saunois, M., and Coauthors, 2016a: The global methane budget 2000–2012. *Earth Syst. Sci. Data*, **8**, 697–751, doi:10.5194/essd-8-697-2016.

——, R. B. Jackson, P. Bousquet, B. Poulter, and J. G. Canadell, 2016b: The growing role of methane in anthropogenic climate change. *Environ. Res. Lett.*, **11**, 120207, doi:10.1088/1748-9326/11/12/120207.

——, and Coauthors, 2017: Variability and quasi-decadal changes in the methane budget over the period 2000-2012. *Atmos. Chem. Phys.*, **17**, 11135–11161, doi:10.5194/acp-17-11135-2017.

Schäfer, K. V. R., R. Tripathee, F. Artigas, T. H. Morin, and G. Bohrer, 2014: Carbon dioxide fluxes of an urban tidal marsh in the Hudson-Raritan estuary. *J. Geophys. Res. Biogeosciences*, **119**, 2065–2081, doi:10.1002/2014JG002703.

Schaller, C., F. Kittler, T. Foken, and M. Göckede, 2018: Characterisation of short-term extreme methane fluxes related to non-turbulent mixing above an Arctic permafrost ecosystem. *Atmos. Chem. Phys. Discuss.*, 1–30, doi:10.5194/acp-2018-277.

Schipper, L. A., J. K. Hobbs, S. Rutledge, and V. L. Arcus, 2014: Thermodynamic theory explains the temperature optima of soil microbial processes and high Q10 values at low temperatures. *Glob. Chang. Biol.*, **20**, 3578–3586, doi:10.1111/gcb.12596.

Schrier-Uijl, A. P., P. S. Kroon, A. Hensen, P. A. Leffelaar, F. Berendse, and E. M. Veenendaal, Comparison of chamber and eddy covariance-based CO2 and CH4 emission estimates in a heterogeneous grass ecosystem on peat. *Agric. For. Meteorol.*, **150**, 825–831, doi:10.1016/j.agrformet.2009.11.007.

Accepted for publication in *Bulletin of the American Meteorological Society.* DOI 10.1175/BAMS-D-18-0268.1.

1151 Shoemaker, J. K., T. F. Keenan, D. Y. Hollinger, and A. D. Richardson, 2014: Forest ecosystem
1152 changes from annual methane source to sink depending on late summer water balance.
1153 *Geophys. Res. Lett.*, **41**, 673–679, doi:10.1002/2013GL058691.
1154 Shurpali, N. J., and S. B. Verma, 1998: Micrometeorological measurements of methane flux in a
1155 Minnesota peatland during two growing seasons. *Biogeochemistry*, **40**, 1–15,
1156 doi:10.1023/A:1005875307146.
1157 Stoy, P. C., G. G. Katul, M. B. S. Siqueira, J.-Y. Juang, H. R. McCarthy, H.-S. Kim, A. C. Oishi,
1158 and R. Oren, 2005: Variability in net ecosystem exchange from hourly to inter-annual time
1159 scales at adjacent pine and hardwood forests: a wavelet analysis. *Tree Physiol.*, **25**, 887–
1160 902, doi:10.1093/treephys/25.7.887.
1161 Sturtevant, C., B. L. Ruddell, S. H. Knox, J. Verfaillie, J. H. Matthes, P. Y. Oikawa, and D.
1162 Baldocchi, 2016: Identifying scale-emergent, nonlinear, asynchronous processes of wetland
1163 methane exchange. *J. Geophys. Res. Biogeosciences*, **121**, 188–204,
1164 doi:10.1002/2015JG003054.
1165 Torrence, C., and G. P. Compo, 1998: A practical guide to wavelet analysis. *Bull. Am. Meteorol.*
1166 *Soc.*, **79**, 61–78, doi:10.1175/1520-0477(1998)079<0061:APGTWA>2.0.CO;2.
1167 Tramontana, G., and Coauthors, 2016: Predicting carbon dioxide and energy fluxes across global
1168 FLUXNET sites with regression algorithms. *Biogeosciences*, **13**, 4291–4313,
1169 doi:10.5194/bg-13-4291-2016.
1170 Treat, C. C., J. L. Bubier, R. K. Varner, and P. M. Crill, 2007: Timescale dependence of
1171 environmental and plant-mediated controls on CH4 flux in a temperate fen. *J. Geophys.*
1172 *Res. Biogeosciences*, **112**, G01014, doi:10.1029/2006JG000210.
1173 Treat, C. C., and Coauthors, 2018a: Tundra landscape heterogeneity, not interannual variability,

Accepted for publication in *Bulletin of the American Meteorological Society.* DOI 10.1175/BAMS-D-18-0268.1.

controls the decadal regional carbon balance in the Western Russian Arctic. *Glob. Chang. Biol.*, **24**, 5188–5204, doi:10.1111/gcb.14421.

——, A. A. Bloom, and M. E. Marushchak, 2018b: Nongrowing season methane emissions-a significant component of annual emissions across northern ecosystems. *Glob. Chang. Biol.*, **24**, 3331–3343, doi:10.1111/gcb.14137.

Tuovinen, J.-P., and Coauthors, 2019: Interpreting eddy covariance data from heterogeneous Siberian tundra: land-cover-specific methane fluxes and spatial representativeness. *Biogeosciences*, **16**, 255–274, doi:10.5194/bg-16-255-2019.

Turetsky, M. R., and Coauthors, 2014: A synthesis of methane emissions from 71 northern, temperate, and subtropical wetlands. *Glob. Chang. Biol.*, **20**, 2183–2197, doi:10.1111/gcb.12580.

Turner, A. J., C. Frankenberg, and E. A. Kort, 2019: Interpreting contemporary trends in atmospheric methane. *Proc. Natl. Acad. Sci.*, **116**, 2805–2813, doi:10.1073/PNAS.1814297116.

Vargas, R., D. D. Baldocchi, M. Bahn, P. J. Hanson, K. P. Hosman, L. Kulmala, J. Pumpanen, and B. Yang, 2011: On the multi-temporal correlation between photosynthesis and soil CO2 efflux: Reconciling lags and observations. *New Phytol.*, **191**, 1006–1017, doi:10.1111/j.1469-8137.2011.03771.x.

Verma, S. B., F. G. Ullman, D. Billesbach, R. J. Clement, J. Kim, and E. S. Verry, 1992: Eddy correlation measurements of methane flux in a northern peatland ecosystem. *Boundary-Layer Meteorol.*, **58**, 289–304, doi:10.1007/BF02033829.

Villarreal, S., M. Guevara, D. Alcaraz-Segura, N. A. Brunsell, D. Hayes, H. W. Loescher, and R. Vargas, 2018: Ecosystem functional diversity and the representativeness of environmental

Accepted for publication in *Bulletin of the American Meteorological Society.* DOI 10.1175/BAMS-D-18-0268.1.

networks across the conterminous United States. *Agric. For. Meteorol.*, **262**, 423–433, doi:10.1016/J.AGRFORMET.2018.07.016.

Vitale, D., M. Bilancia, and D. Papale, 2018: A multiple imputation strategy for eddy covariance data. *J. Environ. Informatics*, doi:10.3808/jei.201800391.

Vuichard, N., and D. Papale, 2015: Filling the gaps in meteorological continuous data measured at FLUXNET sites with ERA-Interim reanalysis. *Earth Syst. Sci. Data*, **7**, 157–171, doi:10.5194/essd-7-157-2015.

Wahlen, M., 1993: The Global Methane Cycle. *Annu. Rev. Earth Planet. Sci.*, **21**, 407–426, doi:10.1146/annurev.earth.21.1.407.

Windham-Myers, L., B. Bergamaschi, F. Anderson, S. Knox, R. Miller, and R. Fujii, 2018: Potential for negative emissions of greenhouse gases (CO2 , CH4 and N2O) through coastal peatland re-establishment: Novel insights from high frequency flux data at meter and kilometer scales. *Environ. Res. Lett.*, **13**, 045005, doi:10.1088/1748-9326/aaae74.

Wolfe, G. M., and Coauthors, 2018: The NASA Carbon Airborne Flux Experiment (CARAFE): instrumentation and methodology. *Atmos. Meas. Tech*, **11**, 1757–1776, doi:10.5194/amt-11-1757-2018.

Wutzler, T., A. Lucas-Moffat, M. Migliavacca, J. Knauer, K. Sickel, L. Šigut, O. Menzer, and M. Reichstein, 2018: Basic and extensible post-processing of eddy covariance flux data with REddyProc. *Biogeosciences Discuss.*, doi:10.5194/bg-2018-56.

Xu, K., S. Metzger, and A. R. Desai, 2017: Upscaling tower-observed turbulent exchange at fine spatio-temporal resolution using environmental response functions. *Agric. For. Meteorol.*, **232**, 10–22, doi:10.1016/J.AGRFORMET.2016.07.019.

Yagi, K., and K. Minami, 1990: Effect of organic matter application on methane emission from

Accepted for publication in *Bulletin of the American Meteorological Society.* DOI 10.1175/BAMS-D-18-0268.1.

some japanese paddy fields. *Soil Sci. Plant Nutr.*, **36**, 599–610, doi:10.1080/00380768.1990.10416797.

Yang, W. H., G. McNicol, Y. A. Teh, K. Estera-Molina, T. E. Wood, and W. L. Silver, 2017: Evaluating the Classical Versus an Emerging Conceptual Model of Peatland Methane Dynamics. *Global Biogeochem. Cycles*, **31**, 1435–1453, doi:10.1002/2017GB005622.

Yvon-Durocher, G., A. P. Allen, D. Bastviken, R. Conrad, C. Gudasz, A. St-Pierre, N. Thanh-Duc, and P. A. del Giorgio, 2014: Methane fluxes show consistent temperature dependence across microbial to ecosystem scales. *Nature*, **507**, 488–491, doi:10.1038/nature13164.

Zona, D., and Coauthors, 2016: Cold season emissions dominate the Arctic tundra methane budget. *Proc. Natl. Acad. Sci.*, **113**, 40–45, doi:10.1073/pnas.1516017113.

Zuur, A. F., E. N. Ieno, N. J. Walker, A. A. Saveliev, and G. M. Smith, 2009: Mixed Effects Modelling for Nested Data. Springer, New York, NY, 101–142.

Accepted for publication in *Bulletin of the American Meteorological Society.* DOI 10.1175/BAMS-D-18-0268.1.

Tables

Table 1. Number of site years and characteristics of CH_4 fluxes (g C m^{-2} y^{-1}) currently included in the database. Fluxes are compared with measurements reported in a recent synthesis of predominantly chamber-based CH_4 flux measurements. Biome type was extracted from Olson et al. (2001) using site coordinates and includes tundra, boreal/taiga, temperate, and tropical/subtropical. Wetland CH_4 emissions differed significantly across biomes, with letters indicating significant differences ($\alpha = 0.05$) among biomes.

Biome	#Site years	Median annual CH_4 flux	25th Percentile	75th Percentile	References
Tundra	10	2.9	1.8	4.2	This study - all sites
	10	2.9[a]	1.8	4.2	This study - wetlands
	31	5.6	1.0	11.4	Treat et al. (2018)† - all sites
	26	6.3	3.0	16.4	Treat et al. (2018) - wetlands
Boreal &	35	8.3	4.1	10.9	This study - all sites
Taiga	30	9.5[ab]	6.0	11.3	This study - wetlands
	68	13.1	3.5	23.7	Treat et al. (2018) - all sites
	67	13.2	3.6	23.7	Treat et al. (2018) - wetlands
Temperate	72	16.4	7.9	35.9	This study - all sites
	47	27.4[b]	10.0	47.3	This study - wetlands
	27	4.3	0.3	41.7	Treat et al. (2018) - all sites
	25	5.3	0.8	42.2	Treat et al. (2018) - wetlands
Tropical &	3	43.2	20.0	46.8	This study - all sites
Subtropical	3	43.2[ab]	20.0	46.8	This study - wetlands
	--	--	--	--	Treat et al. (2018) - all sites
	--	--	--	--	Treat et al. (2018) - wetlands

† Note that similar to our tower only dataset, values from Treat et al. (2018) represent measured annual fluxes derived from a smaller dataset where measurements were made in the growing season and non-growing season.

Accepted for publication in *Bulletin of the American Meteorological Society.* DOI 10.1175/BAMS-D-18-0268.1.

Appendix A: Sites currently included in the database

Table A1. Characteristics of sites currently included in the database. Ecosystem type is based on the classification of Olefeldt *et al.* (2013) and Treat *et al.* (2018). Biome was based on the classification of Olson *et al.* (2001) and extracted using site coordinates. Vegetation type was based on the International Geosphere-Biosphere Programme (IGBP) definition. Salinity regime includes freshwater (FW) or saltwater (SW) wetlands. Disturbance is based on the classification of Turetsky *et al.* (2014). Data from all sites are publicly available, primarily through Ameriflux and the European Database Cluster, and in a few cases, through other databases/repositories. Site DOIs are specified where applicable.

Site ID	Site Name	Country	Lat	Long	Biome	IGBP	Ecosystem Type	Salinity	Wetland Disturbance	Site PI	data DOI/Location
US-ICs	Wet sedge tundra	USA	68.606	-149.311	Tundra	WET	Wet tundra	FW	Undisturbed	Eugenie Euskirchen	doi: 10.17190/AMF/1246130
SE-St1	Stordalen grassland (Mire)	Sweden	68.350	19.050	Tundra	WET	Fen	FW	Undisturbed	Thomas Friborg	European Fluxes Database Cluster
SE-Sto	Stordalen Palsa Bog	Sweden	68.356	19.050	Tundra	WET	Bog	FW	Undisturbed	Thomas Friborg	European Fluxes Database Cluster
RU-Vrk	Seida/Vorkuta	Russia	67.055	62.940	Tundra	WET	Wet tundra	FW	Undisturbed	Thomas Friborg	European Fluxes Database Cluster
RU-Ch2	Chersky reference	Russia	68.617	161.351	Tundra	WET	Wet tundra	FW	Undisturbed	Matthias Goeckede	European Fluxes Database Cluster
RU-Che	Chersky	Russia	68.613	161.341	Tundra	WET	Wet tundra	FW	Drying	Matthias Goeckede	European Fluxes Database Cluster
RU-SAM	Samoylov	Russia	72.374	126.496	Tundra	WET	Wet tundra	FW	Undisturbed	Torsten Sachs	European Fluxes Database Cluster

Accepted for publication in *Bulletin of the American Meteorological Society.* DOI 10.1175/BAMS-D-18-0268.1.

US-NGB	NGEE Barrow	USA	71.280	-156.609	Tundra	WET	Wet tundra	FW	Undisturbed	Margaret Torn	doi: 10.17190/AMF/1436326
US-Beo	Barrow	USA	71.281	-156.612	Tundra	WET	Wet tundra	FW	Undisturbed	Donatella Zona	Ameriflux
US-Bes	Barrow	USA	71.281	-156.596	Tundra	WET	Wet tundra	FW	Undisturbed	Donatella Zona	Ameriflux
US-Atq	Atqasuk	USA	70.470	-157.409	Tundra	WET	Wet tundra	FW	Undisturbed	Donatella Zona	doi:10.17190/AMF/1246029
US-Ivo	Ivotuk	USA	68.486	-155.750	Tundra	WET	Wet tundra	FW	Undisturbed	Donatella Zona	doi:10.17190/AMF/1246067
--	Black spruce forest	USA	64.700	-148.320	Boreal Forests/Taiga	ENF	Upland	--	--	Eugenie Euskirchen	http://www.lter.uaf.edu/data/data-detail/id/708
--	Rich Fen	USA	64.704	-148.313	Boreal Forests/Taiga	WET	Fen	FW	Undisturbed	Eugenie Euskirchen	http://www.lter.uaf.edu/data/data-detail/id/708
--	Thermokarst collapse scar bog	USA	64.700	-148.320	Boreal Forests/Taiga	WET	Bog	FW	Undisturbed	Eugenie Euskirchen	http://www.lter.uaf.edu/data/data-detail/id/708
FI-Lom	Lompolojankka	Finland	67.997	24.209	Boreal Forests/Taiga	WET	Fen	FW	Undisturbed	Annalea Lohila	European Fluxes Database Cluster
SE-Deg	Degero	Sweden	64.182	19.557	Boreal Forests/Taiga	WET	Fen	FW	Undisturbed	Matthias Peichl, Mats Nilsson	European Fluxes Database Cluster
CA-SCC	Scotty Creek - Peat plateau/collapse scar	Canada	61.308	-121.299	Boreal Forests/Taiga	ENF	Peat plateau	FW	--	Oliver Sonnentag	doi:10.17190/AMF/1480303
CA-SCB	Scotty Creek Bog	Canada	61.309	-121.299	Boreal Forests/Taiga	WET	Bog	FW	Undisturbed	Oliver Sonnentag	Ameriflux
US-NGC	NGEE Arctic Council	USA	64.861	-163.701	Boreal Forests/Taiga	WET	Wet tundra	FW	Undisturbed	Margaret Torn	Ameriflux

Accepted for publication in *Bulletin of the American Meteorological Society.* DOI 10.1175/BAMS-D-18-0268.1.

US-Uaf	University of Alaska, Fairbanks	USA	64.866	-147.856	Boreal Forests/Taiga	WET	Bog	FW	Undisturbed	Masahito Ueyama	doi:10.17190/AMF/1480322
FI-Sii	Siikaneva I (FI-Sii)	Finland	61.833	24.193	Boreal Forests/Taiga	WET	Fen	FW	Undisturbed	Timo Vesala & Ivan Mammarella	European Fluxes Database Cluster
FI-Si2	Siikaneva II	Finland	61.837	24.170	Boreal Forests/Taiga	WET	Bog	FW	Undisturbed	Timo Vesala & Ivan Mammarella	European Fluxes Database Cluster
US-Myb	Mayberry Wetland	USA	38.050	-121.765	Temperate	WET	Marsh	FW	Wetting	Dennis Baldocchi	doi: 10.17190/AMF/1246139
US-Sne	Sherman Island Restored Wetland	USA	38.037	-121.755	Temperate	WET	Marsh	FW	Wetting	Dennis Baldocchi	doi: 10.17190/AMF/1418684
US-Tw1	Twitchell West Pond Wetland	USA	38.107	-121.647	Temperate	WET	Marsh	FW	Wetting	Dennis Baldocchi	doi: 10.17190/AMF/1246147
US-Tw4	Twitchell East End Wetland	USA	38.103	-121.641	Temperate	WET	Marsh	FW	Wetting	Dennis Baldocchi	doi: 10.17190/AMF/1246148
US-Twt	Twitchell Rice	USA	38.109	-121.653	Temperate	CRO - Rice	Rice	FW	--	Dennis Baldocchi	doi: 10.17190/AMF/1246151
US-Bi2	Bouldin Island corn	USA	38.109	-121.535	Temperate	CRO - Other	Drained/Agricultural wetland	FW	Drying	Dennis Baldocchi	doi: 10.17190/AMF/1419513
US-Bi1	Bouldin Island Alfalfa	USA	38.102	-121.504	Temperate	CRO - Other	Drained/Agricultural wetland	FW	Drying	Dennis Baldocchi	doi:10.17190/AMF/1480317

Accepted for publication in *Bulletin of the American Meteorological Society.* DOI 10.1175/BAMS-D-18-0268.1.

US-Snd	Sherman Island	USA	38.037	-121.754	Temperate	CRO - Other	Drained/Agricultural wetland	FW	Drying	Dennis Baldocchi	doi: 10.17190/AMF/1246094
US-OWC	Old Woman Creek	USA	41.380	-82.512	Temperate	WET	Marsh	FW	Undisturbed	Gil Bohrer	doi: 10.17190/AMF/1246094
US-ORv	Olentangy River Wetland Research Park	USA	40.020	-83.018	Temperate	WET	Marsh	FW	Undisturbed	Gil Bohrer	doi:10.17190/AMF/1246135
NZ-Kop	Kopuatai	New Zealand	-37.388	175.554	Temperate	WET	Bog	FW	Undisturbed	Dave Campbell	https://researchcommons.waikato.ac.nz/handle/10289/11393
IT-Cas	Castellaro	Italy	45.070	8.718	Temperate	CRO - Rice	Rice	FW	--	Alessandro Cescatti	European Fluxes Database Cluster
US-WPT	Winous Point North Marsh	USA	41.465	-82.996	Temperate	WET	Marsh	FW	Wetting	Jiquan Chen & Housen Chu	doi: 10.17190/AMF/1246155
US-CRT	Curtice Walter-Berger cropland	USA	41.628	-83.347	Temperate	CRO - Other	Upland	--	--	Jiquan Chen & Housen Chu	doi: 10.17190/AMF/1246156
US-Los	Lost Creek	USA	46.083	-89.979	Temperate	WET	Fen	FW	Undisturbed	Ankur Desai	doi: 10.17190/AMF/1246071
JP-Mse	Mase paddy flux site (MSE)	Japan	36.054	140.027	Temperate	CRO - Rice	Rice	FW	--	Akira Miyata	European Fluxes Database Cluster
JP-Swl	Suwa Lake Site	japan	36.047	138.108	Temperate	WAT	Waterbody	FW	Undisturbed	Hiroki Iwata	European Fluxes Database Cluster
IT-BCi	Borgo Cioffi	Italy	40.524	14.957	Temperate	CRO - Other	Upland	--	--	Vincenzo Magliulo	European Fluxes Database Cluster
--	Hongyuan	China	32.800	102.550	Temperate	GRA	Upland	--	--	Shuli Niu	European Fluxes Database Cluster

Accepted for publication in *Bulletin of the American Meteorological Society.* DOI 10.1175/BAMS-D-18-0268.1.

US-NC4	NC Alligator River	USA	35.788	-75.904	Temperate	WET	Swamp	FW	Undisturbed	Asko Noormets	doi:10.17190/AMF/1480314
DE-SfN	Schechenfilz Nord	Germany	47.806	11.328	Temperate	WET	Bog	FW	Undisturbed	Hans Peter Schmid	European Fluxes Database Cluster
US-Ho1	Howland Forest (main tower)	USA	45.204	-68.740	Temperate	ENF	Upland	--	--	Andrew Richardson	doi:10.17190/AMF/1246061
US-HRA	Humnoke Farm Rice Field AWD, United States	USA	34.585	-91.752	Temperate	CRO - Rice	Rice	FW	--	Benjamin Runkle	Ameriflux
US-HRC	Humnoke Farm Rice Field conventional, United States	USA	34.589	-91.752	Temperate	CRO - Rice	Rice	FW	--	Benjamin Runkle	Ameriflux
KR-CRK	Cheorwon Rice paddy	South Korea	38.201	127.251	Temperate	CRO - Rice	Rice	FW	--	Youngryel Ryu & Minseok Kang	European Fluxes Database Cluster
DE-Zrk	Zarnekow	Germany	53.876	12.889	Temperate	WET	Fen	FW	Wetting	Torsten Sachs	European Fluxes Database Cluster
DE-Dgw	Dagowsee	Germany	53.151	13.054	Temperate	WAT	Waterbody	FW	Undisturbed	Torsten Sachs	European Fluxes Database Cluster
US-MRM	Marsh Resource Meadowlands Mitigation Bank	USA	40.816	-74.044	Temperate	WET	Salt Marsh	SW	Wetting	Karina Schäfer	Ameriflux
--	Bog Lake peatland	USA	47.530	-93.470	Temperate	WET	Fen	FW	Undisturbed	Shahi Verma	Ameriflux

Accepted for publication in *Bulletin of the American Meteorological Society.* DOI 10.1175/BAMS-D-18-0268.1.

--	MacArthur Agro-Ecology Research Center	USA	27.163	-81.187	Temperate	CRO - Other	Drained/Agricultural wetland	FW	Drying	Jed Sparks & Samuel Chamberlain	Ameriflux
JP-BBY	Bibai bog	Japan	43.323	141.811	Temperate	WET	Bog	FW	Undisturbed	Masahito Ueyama	European Fluxes Database Cluster
US-StJ	St Jones Reserve	USA	39.088	-75.437	Temperate	WET	Salt Marsh	SW	Undisturbed	Rodrigo Vargas	doi:10.17190/AMF/1480316
US-Srr	Suisun marsh - Rush Ranch	USA	38.201	-122.026	Temperate	WET	Salt Marsh	SW	Undisturbed	Lisamarie Windham-Myers	doi:10.17190/AMF/1418685
AT-Neu	Neustift	Austria	47.117	11.318	Temperate	GRA	Upland	--	--	Georg Wohlfahrt	European Fluxes Database Cluster
US-LA2	Salvador WMA Freshwater Marsh	USA	29.859	-90.287	Tropical & Subtropical	WET	Marsh	FW	Undisturbed	Ken Krauss	Ameriflux
US-LA1	Pointe-aux-Chenes Brackish Marsh	USA	29.501	-90.445	Tropical & Subtropical	WET	Salt Marsh	SW	Undisturbed	Ken Krauss	Ameriflux
MY-MLM	Maludam	Malaysia	1.454	111.149	Tropical & Subtropical	WET	Swamp	FW	Undisturbed	Angela Tang	https://doi.org/10.5281/zenodo.1161966

1250

Accepted for publication in *Bulletin of the American Meteorological Society.* DOI 10.1175/BAMS-D-18-0268.1.

Figure Caption List

Figure 1. Location of the 200 tower sites that report eddy covariance CH_4 flux measurements worldwide. Triangles indicate sites from which data are included in this manuscript, with circles indicating additional flux towers measuring CH_4 emissions. The colors of the markers represent the vegetation type based on the International Geosphere-Biosphere Programme (IGBP) definition. See Table S1 for a list of sites, their characteristics, and years of operation. Sites are overlaid over a map of the differences between the average CH_4 emissions over 2000-2010 between top-down and bottom-up wetland CH_4 estimates. Top-down estimates are represented by the natural fluxes inventoried in NOAA's CarbonTracker (https://www.esrl.noaa.gov/gmd/ccgg/carbontracker-ch4/). Bottom-up emissions were produced from an ensemble of 11 Earth System Models simulations (Poulter et al. 2017).

Figure 2. Distribution of sites by mean annual air temperature and precipitation. Tower locations are shown as circles or triangles, with vegetation type in color based on the IGBP definitions (CRO = Croplands; DBF = Deciduous Broadleaf Forests; EBF = Evergreen Broadleaf Forests; ENF = Evergreen Needleleaf Forests; GRA = Grasslands; MF = Mixed Forests; URB = Urban and Built-Up Lands; WAT = Water Bodies; WET = Permanent Wetlands). Gray dots represent annual mean temperature and total precipitation from the CRU TS 3.10 gridded climate dataset over the entire land mass (Harris et al. 2014), whereas blue dots represent grid cells with >25% wetland fraction as estimated using the Global Lakes and Wetlands Database (Lehner and Döll 2004). Temperature and precipitation grid cells included in this figure were averaged from 1981 to 2011, at 0.5° resolution.

Figure 3. (a) Probability density function, and (b) cumulative frequency distribution of half-hourly CH_4 flux (F_{CH4}) data for sites currently included in the database (60 sites) aggregated by biome. Thin lines represent individual sites, whereas thicker lines present sites aggregated by biome. All cases are approximated by kernel density estimation. Note that whereas the x-axis is scaled between -50 and 900 nmol m^{-2} s^{-1} for visualization purposes, some CH_4 fluxes exceed this range.

Figure 4. (a) Histogram of annual CH_4 fluxes (F_{CH4}; g C m^{-2} y^{-1}) measured with eddy covariance and published in the synthesis by Baldocchi (2014), and (b) histogram of annual CH_4 fluxes including additional site years of data estimated from the 60 sites listed in Table A1.

Figure 5. Annual CH_4 fluxes (F_{CH4}; g C m^{-2} y^{-1}) among ecosystem types for the 60 sites currently included in the database (Table A1). Letters indicate significant differences ($\alpha = 0.05$) among ecosystem types. Median value, first and third quartiles are presented in the boxes, and dots represent outliers, which are defined as observations more than 1.5-times the interquartile range away from the top or bottom of the box.

Figure 6. Relationship between annual CH_4 flux (F_{CH4}) and (a) mean annual air temperature (T_{MAT}) ($\chi^2 = 36.7$, $df = 1$, $p < 0.001$), (b) mean annual soil temperature (T_{MST}) ($\chi^2 = 32.3$, $df = 1$, $p < 0.001$) for freshwater wetlands, and (c) mean water table depth (WTD). While there was no significant relationship between mean annual WTD and annual CH_4 flux across all sites, there

Accepted for publication in *Bulletin of the American Meteorological Society.* DOI 10.1175/BAMS-D-18-0268.1.

was a significant relationship if we consider only sites where WTD was below the soil surface for part or all of the year (solid circles) ($\chi^2 = 5.6$, $df = 1$, $p < 0.05$). Open circles in (c) indicate CH_4 emissions for permanently inundated sites. (d) shows the temperature dependence of the annual CH_4:ER ratio ($\chi^2 = 12.0$, $df = 1$, $p < 0.001$). Lines represent the fitted values for the population.

Figure 7. Variance of CH_4 flux (F_{CH4}) wavelet coefficients across time scales, as a percentage of the total variance, averaged by wetland type. Error bars represent the standard error. Note that only ecosystem types with at least 6 sites are shown here, including bogs, fens, freshwater (FW) marshes, rice paddies, and wet tundra.

Figure 8. Relationship between the correlation coefficient (r^2) calculated from the median ANN prediction and observed CH_4 fluxes at each site and the percentage of total variance at diel and seasonal scales ($r^2 = 0.69$, $p < 0.001$). Each site is color coded by ecosystem type. Size of the dots are proportional to the magnitude of mean CH_4 flux, where flux magnitude was aggregated into 10 bins for plotting.

Figure 9. (a) Scaling of F_{CH4} random flux measurement error ($\sigma(\delta)$) with flux magnitude for all sites with a significant linear relationship between random error and flux magnitude (95% of all sites). Data at each site were placed into 10 bins (Oikawa et al. 2017). (b) Scaling of F_{CH4} random flux measurement error, characterized by the standard deviation of the double-exponential distribution ($\sigma(\delta)$), with mean flux magnitude across sites. There was a significant linear relationship between $\sigma(\delta)$ and the magnitude of mean CH_4 flux ($\sigma(\delta) = 0.5 \times F_{CH4} + 5.9$, $r^2 = 0.86$, $p < 0.001$), even when excluding the two highest CH_4-emitting sites ($\sigma(\delta) = 0.4 \times F_{CH4} + 11.3$, $r^2 = 0.46$, $p < 0.001$). Note that circle represent sites with open-path CH_4 analyzers while asterisks represent sites with closed-path sensors.

Figure 10. (a) Histogram of total random error (g C m^{-2} y^{-1}) in annual CH_4 flux at 95% confidence, where count refers to the number of site years of measurements. The cumulative gap-filling and random measurement uncertainties of gap-filled and original values were added in quadrature to estimate the total random uncertainty at each site. (b) Relationship between annual CH_4 flux (g C m^{-2} y^{-1}) and relative error (i.e. total random error divided by flux magnitude; %).

Figure 11. Footprint climatology for a eutrophic shallow lake on a formerly drained fen in Germany (Zarnekow; DE-Zrk) illustrating the importance of footprint analysis for the interpretation of EC measurements of CH_4. Here we used two footprint models, including the model of Kormann & Meixner (2001) (2001) (yellow) and Kljun et al. (2015) (white). The footprint climatology was calculated by aggregating all half-hour footprints within a year. The dashed lines enclose the areas aggregating to 80% of source areas, while solid lines enclose the 50% of source areas.

Accepted for publication in *Bulletin of the American Meteorological Society.* DOI 10.1175/BAMS-D-18-0268.1.

Figures

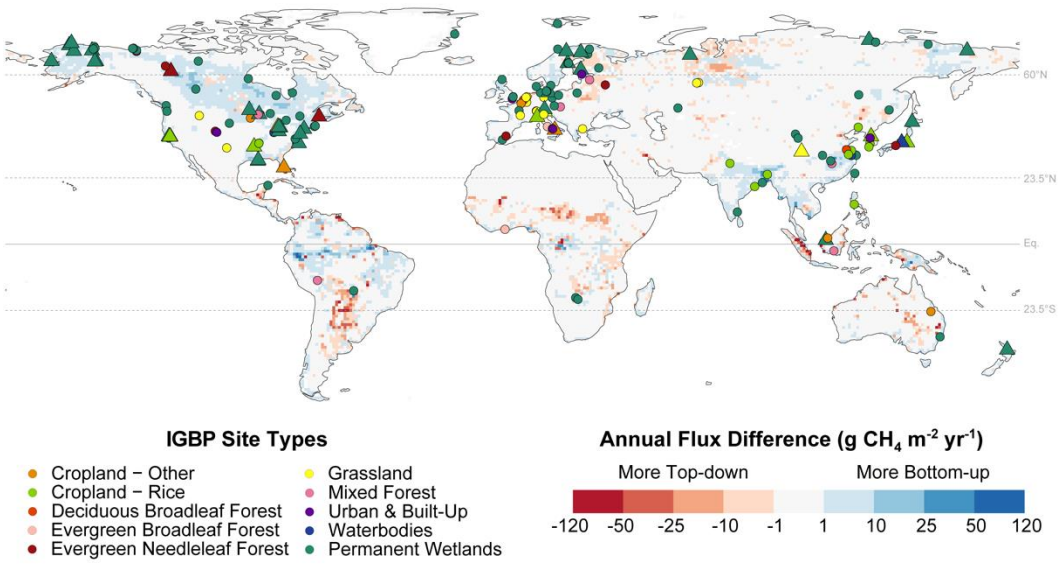

Figure 1. Location of the 200 tower sites that report eddy covariance CH_4 flux measurements worldwide. Triangles indicate sites from which data are included in this manuscript, with circles indicating additional flux towers measuring CH_4 emissions. The colors of the markers represent the vegetation type based on the International Geosphere-Biosphere Programme (IGBP) definition. See Table S1 for a list of sites, their characteristics, and years of operation. Sites are overlaid over a map of the differences between the average CH_4 emissions over 2000-2010 between top-down and bottom-up wetland CH_4 estimates. Top-down estimates are represented by the natural fluxes inventoried in NOAA's CarbonTracker (https://www.esrl.noaa.gov/gmd/ccgg/carbontracker-ch4/). Bottom-up emissions were produced from an ensemble of 11 Earth System Models simulations (Poulter et al. 2017).

Accepted for publication in *Bulletin of the American Meteorological Society.* DOI 10.1175/BAMS-D-18-0268.1.

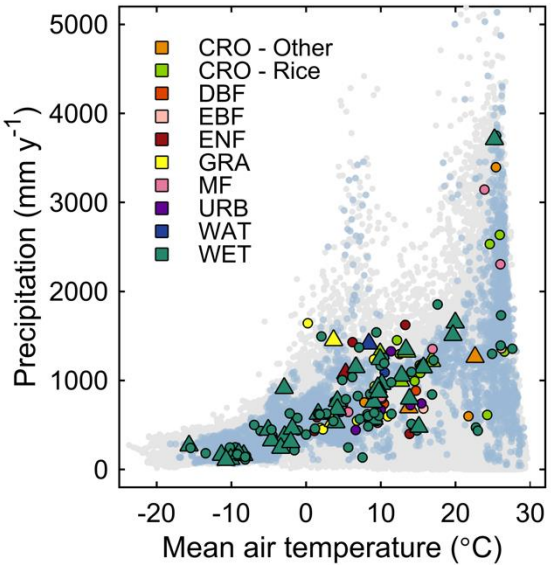

Figure 2. Distribution of sites by mean annual air temperature and precipitation. Tower locations are shown as circles or triangles, with vegetation type in color based on the IGBP definitions (CRO = Croplands; DBF = Deciduous Broadleaf Forests; EBF = Evergreen Broadleaf Forests; ENF = Evergreen Needleleaf Forests; GRA = Grasslands; MF = Mixed Forests; URB = Urban and Built-Up Lands; WAT = Water Bodies; WET = Permanent Wetlands). Gray dots represent annual mean temperature and total precipitation from the CRU TS 3.10 gridded climate dataset over the entire land mass (Harris et al. 2014), whereas blue dots represent grid cells with >25% wetland fraction as estimated using the Global Lakes and Wetlands Database (Lehner and Döll 2004). Temperature and precipitation grid cells included in this figure were averaged from 1981 to 2011, at 0.5° resolution.

Accepted for publication in *Bulletin of the American Meteorological Society.* DOI 10.1175/BAMS-D-18-0268.1.

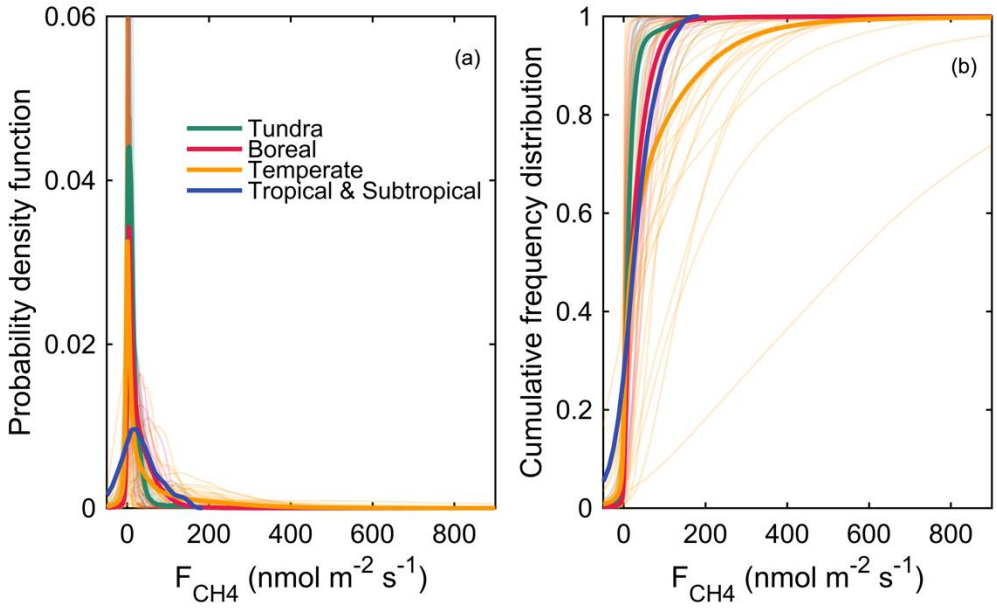

Figure 3. (a) Probability density function, and (b) cumulative frequency distribution of half-hourly CH_4 flux (F_{CH4}) data for sites currently included in the database (60 sites) aggregated by biome. Thin lines represent individual sites, whereas thicker lines present sites aggregated by biome. All cases are approximated by kernel density estimation. Note that whereas the x-axis is scaled between -50 and 900 nmol m^{-2} s^{-1} for visualization purposes, some CH_4 fluxes exceed this range.

Accepted for publication in *Bulletin of the American Meteorological Society.* DOI 10.1175/BAMS-D-18-0268.1.

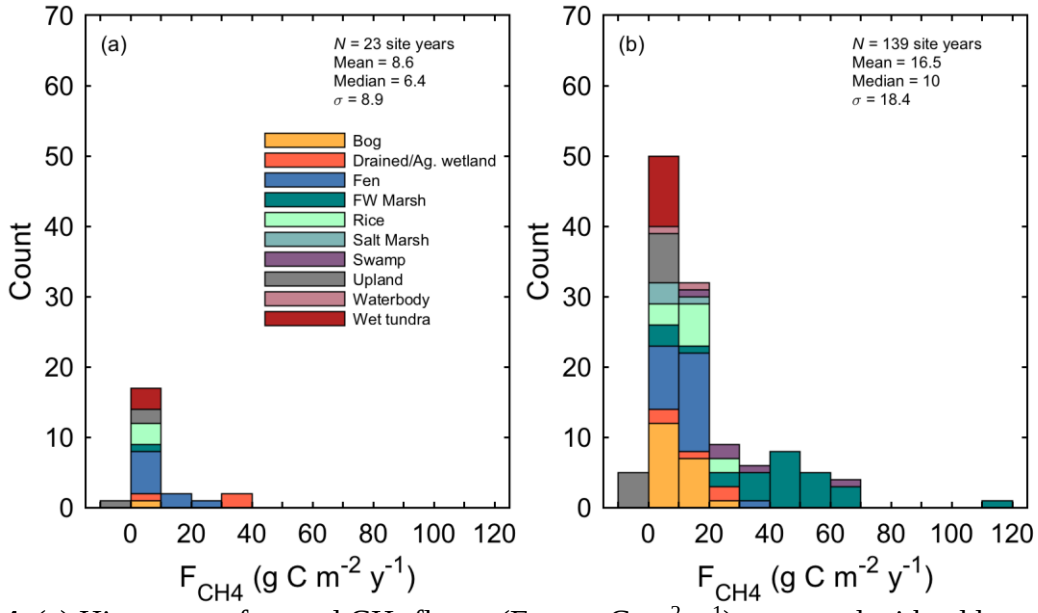

Figure 4. (a) Histogram of annual CH_4 fluxes (F_{CH4}; g C m^{-2} y^{-1}) measured with eddy covariance and published in the synthesis by Baldocchi (2014), and (b) histogram of annual CH_4 fluxes including additional site years of data estimated from the 60 sites listed in Table A1.

Accepted for publication in *Bulletin of the American Meteorological Society.* DOI 10.1175/BAMS-D-18-0268.1.

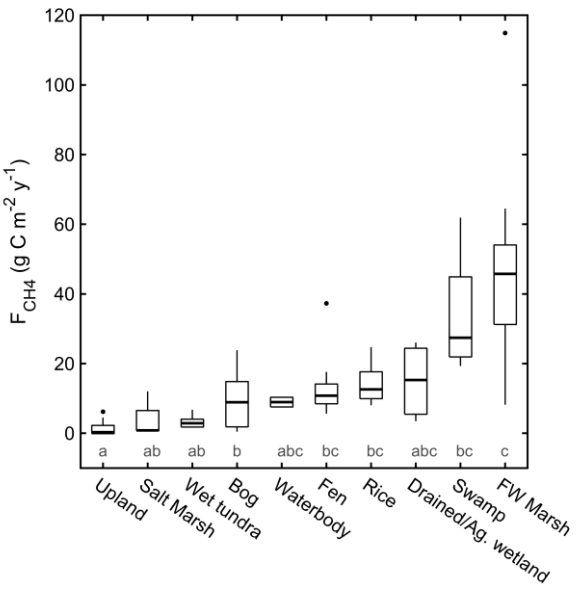

Figure 5. Annual CH_4 fluxes (F_{CH4}; g C m^{-2} y^{-1}) among ecosystem types for the 60 sites currently included in the database (Table A1). Letters indicate significant differences ($\alpha = 0.05$) among ecosystem types. Median value, first and third quartiles are presented in the boxes, and dots represent outliers, which are defined as observations more than 1.5-times the interquartile range away from the top or bottom of the box.

Accepted for publication in *Bulletin of the American Meteorological Society.* DOI 10.1175/BAMS-D-18-0268.1.

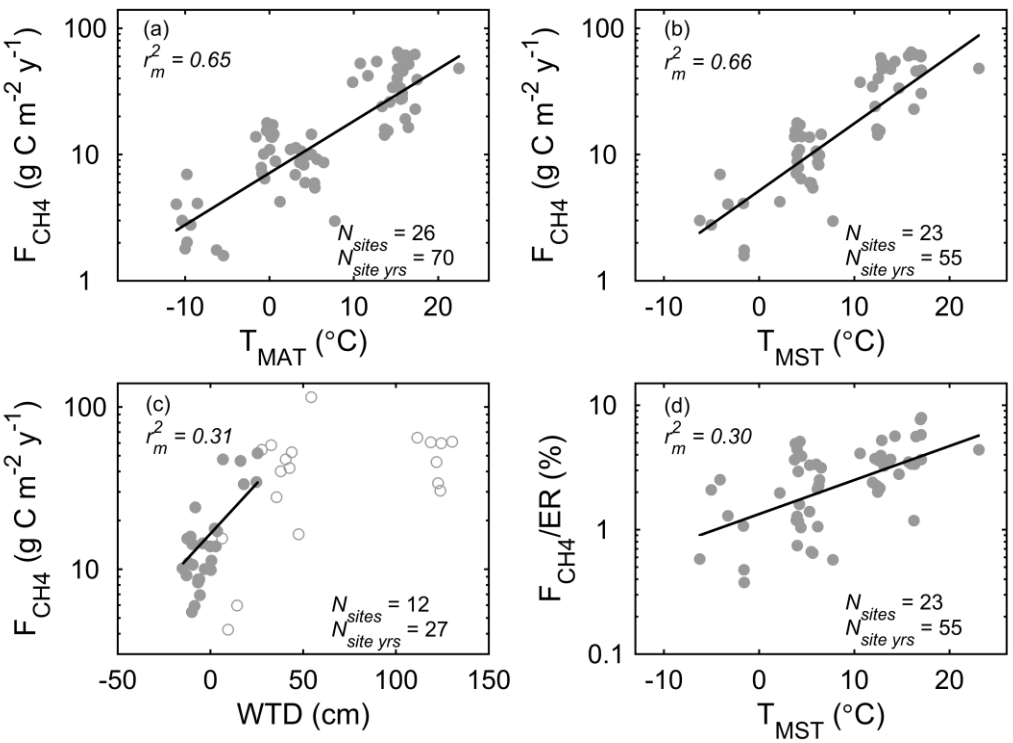

Figure 6. Relationship between annual CH_4 flux (F_{CH4}) and (a) mean annual air temperature (T_{MAT}) (χ^2 = 36.7, *df* = 1, $p < 0.001$), (b) mean annual soil temperature (T_{MST}) (χ^2 = 32.3, *df* = 1, $p < 0.001$) for freshwater wetlands, and (c) mean water table depth (WTD). While there was no significant relationship between mean annual WTD and annual CH_4 flux across all sites, there was a significant relationship if we consider only sites where WTD was below the soil surface for part or all of the year (solid circles) (χ^2 = 5.6, *df* = 1, $p < 0.05$). Open circles in (c) indicate CH_4 emissions for permanently inundated sites. (d) shows the temperature dependence of the annual CH_4:ER ratio (χ^2 = 12.0, *df* = 1, $p < 0.001$). Lines represent the fitted values for the population.

Accepted for publication in *Bulletin of the American Meteorological Society.* DOI 10.1175/BAMS-D-18-0268.1.

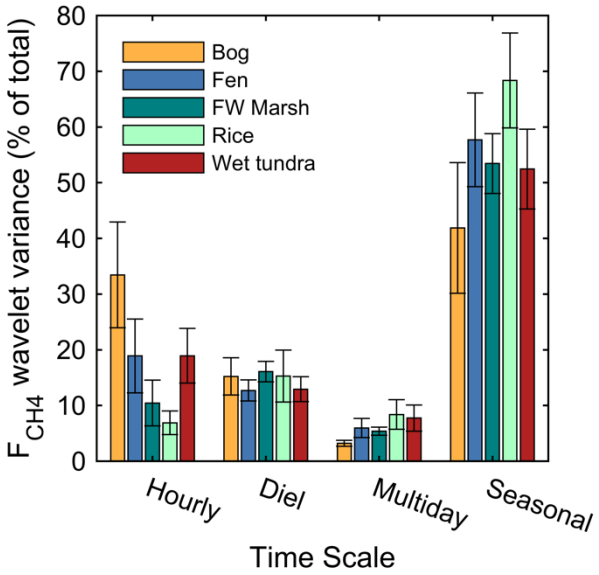

Figure 7. Variance of CH_4 flux (F_{CH4}) wavelet coefficients across time scales, as a percentage of the total variance, averaged by wetland type. Error bars represent the standard error. Note that only ecosystem types with at least 6 sites are shown here, including bogs, fens, freshwater (FW) marshes, rice paddies, and wet tundra.

Accepted for publication in *Bulletin of the American Meteorological Society.* DOI 10.1175/BAMS-D-18-0268.1.

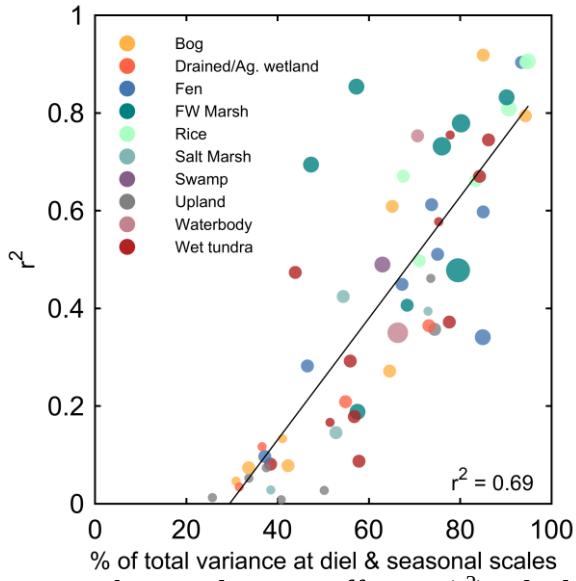

Figure 8. Relationship between the correlation coefficient (r^2) calculated from the median ANN prediction and observed CH_4 fluxes at each site and the percentage of total variance at diel and seasonal scales ($r^2 = 0.69$, $p < 0.001$). Each site is color coded by ecosystem type. Size of the dots are proportional to the magnitude of mean CH_4 flux, where flux magnitude was aggregated into 10 bins for plotting.

Accepted for publication in *Bulletin of the American Meteorological Society.* DOI 10.1175/BAMS-D-18-0268.1.

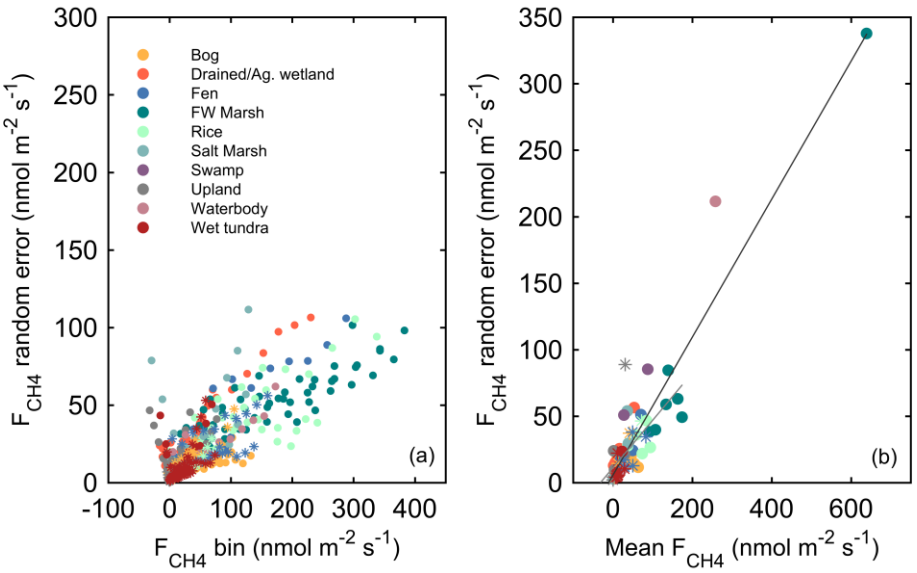

Figure 9. (a) Scaling of F_{CH4} random flux measurement error ($\sigma(\delta)$) with flux magnitude for all sites with a significant linear relationship between random error and flux magnitude (95% of all sites). Data at each site were placed into 10 bins (Oikawa et al. 2017). (b) Scaling of F_{CH4} random flux measurement error, characterized by the standard deviation of the double-exponential distribution ($\sigma(\delta)$), with mean flux magnitude across sites. There was a significant linear relationship between $\sigma(\delta)$ and the magnitude of mean CH_4 flux ($\sigma(\delta) = 0.5 \times F_{CH4} + 5.9$, $r^2 = 0.86$, $p < 0.001$), even when excluding the two highest CH_4-emitting sites ($\sigma(\delta) = 0.4 \times F_{CH4} + 11.3$, $r^2 = 0.46$, $p < 0.001$). Note that circle represent sites with open-path CH_4 analyzers while asterisks represent sites with closed-path sensors.

Accepted for publication in *Bulletin of the American Meteorological Society.* DOI 10.1175/BAMS-D-18-0268.1.

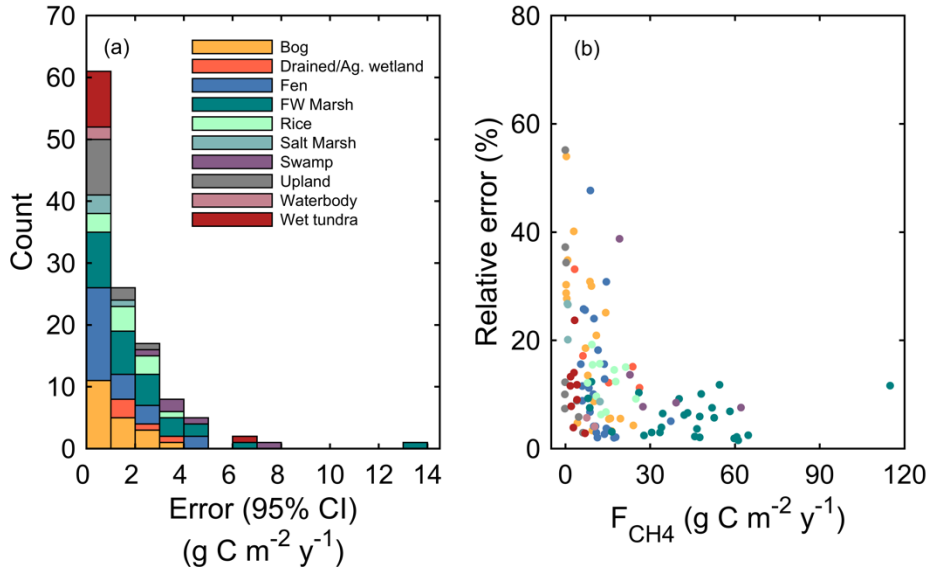

Figure 10. (a) Histogram of total random error (g C m^{-2} y^{-1}) in annual CH_4 flux at 95% confidence, where count refers to the number of site years of measurements. The cumulative gap-filling and random measurement uncertainties of gap-filled and original values were added in quadrature to estimate the total random uncertainty at each site. (b) Relationship between annual CH_4 flux (g C m^{-2} y^{-1}) and relative error (i.e. total random error divided by flux magnitude; %).

Accepted for publication in *Bulletin of the American Meteorological Society.* DOI 10.1175/BAMS-D-18-0268.1.

1422

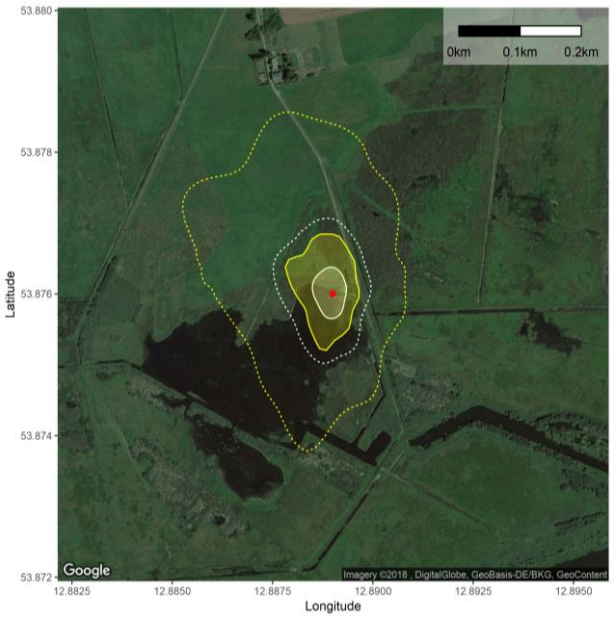

1423

1424 **Figure 11**. Footprint climatology for a eutrophic shallow lake on a formerly drained fen in
1425 Germany (Zarnekow; DE-Zrk) illustrating the importance of footprint analysis for the
1426 interpretation of EC measurements of CH_4. Here we used two footprint models, including the
1427 model of Kormann & Meixner (2001) (2001) (yellow) and Kljun et al. (2015) (white). The
1428 footprint climatology was calculated by aggregating all half-hour footprints within a year. The
1429 dashed lines enclose the areas aggregating to 80% of source areas, while solid lines enclose the
1430 50% of source areas.

Accepted for publication in *Bulletin of the American Meteorological Society.* DOI 10.1175/BAMS-D-18-0268.1.